Geochemistry Geophysics Geosystems G3

Article
Volume 14, Number 10
18 October 2013
doi: 10.1002/ggge.20272
ISSN: 1525-2027

Published by AGU and the Geochemical Society

The influence of high-latitude flux lobes on the Holocene paleomagnetic record of IODP Site U1305 and the northern North Atlantic

Joseph S. Stoner
College of Earth, Ocean, and Atmospheric Sciences, Oregon State University, 104 CEOAS Admin Bldg., Corvallis, Oregon 97331-5503 USA

James E. T. Channell
Department of Geological Sciences, University of Florida, Gainesville, Florida, USA

Alain Mazaud
Laboratoire des Sciences du Climat et de l'Environnement (LSCE)CNRS, Domaine du CNRS, Avenue de la Terrasse, Gif-sur-Yvette, France

Sarah E. Strano
College of Earth, Ocean, and Atmospheric Sciences, Oregon State University, Corvallis, Oregon, USA

Chuang Xuan
College of Earth, Ocean, and Atmospheric Sciences, Oregon State University, Corvallis, Oregon, USA

Now at National Oceanography Centre Southampton, School of Ocean and Earth Science, University of Southampton, Southampton, UK

[1] Paleomagnetic analysis and radiocarbon dating of an expanded Holocene deep-sea sediment sequence recovered by Integrated Ocean Drilling Program (IODP) Expedition 303 from Labrador Sea Site U1305 (Lat.: 57°28.5 N, Long.: 48°31.8 W, water depth 3459 m) provides insights into mechanisms that drive both paleomagnetic secular variation (PSV) and magnetization acquisition in deep-sea sediments. Seventeen radiocarbon dates on planktonic foraminifera define postglacial (ca. 8 ka) sedimentation rates as ranging from 35 to $>$ 90 cm/kyr. Alternating field (AF) demagnetization of u-channel samples show that these homogeneous sediments preserve a strong, stable, and consistently well-defined component magnetization. Normalized remanence records pass reliability criteria for relative paleointensity (RPI) estimates. Assuming that the age of magnetization is most accurately defined by well dated PSV records with the highest sedimentation rates, allows us to estimate and correct for temporal offsets at Site U1305 interpreted to result from postdepositional remanence acquisition at a depth of $\sim$20 cm. Comparisons indicate that the northern North Atlantic PSV and RPI records are more consistent with European than North American records, and the evolution of virtual geomagnetic poles (VGP) are temporally and longitudinally similar to global reconstructions, though with much larger latitudinal variation. The largest deviations from a geocentric axial dipole (GAD) are observed during times of the highest intensities, in contrast to the usual assumption. These observations are consistent with the idea that PSV in the North Atlantic and elsewhere during the Holocene results from temporal oscillations of high-latitude flux concentrations at a few recurrent locations.

Components: 13,704 words, 13 figures, 3 tables.

Keywords: paleomagnetism; North Atlantic; paleointensity.

Index Terms: 1522 Paleomagnetic secular variation: Geomagnetism and Paleomagnetism; 1521 Paleointensity: Geomagnetism and Paleomagnetism; 1512 Environmental magnetism: Geomagnetism and Paleomagnetism; 3022 Marine sediments: processes and transport: Marine Geology and Geophysics; 1115 Radioisotope geochronology: Geochronology.

Received 21 March 2013; **Revised** 5 September 2013; **Accepted** 16 September 2013; **Published** 18 October 2013.

Stoner, J. S., J. E. T. Channell, A. Mazaud, S. E. Strano, and C. Xuan (2013), The influence of high-latitude flux lobes on the Holocene paleomagnetic record of IODP Site U1305 and the northern North Atlantic, *Geochem. Geophys. Geosyst.*, *14*, 4623–4646, doi:10.1002/ggge.20272.

1. Introduction

[2] Paleomagnetic secular variation (PSV) data derived from geological and archeological materials have extended our knowledge of geomagnetic field variability over timescales of 10^3 years and longer [e.g., *Merrill et al*., 1996]. Continuous spherical harmonic models (CSHM) using PSV data provide a useful tool for extending historical assessments of the space/time structure of the geomagnetic field [*Korte and Constable*, 2003, 2005, 2011; *Korte et al*., 2005, 2009, 2011]. Although historical observations indicate persistent high-latitude regions of concentrated nonaxisymmetric flux [e.g., *Bloxham and Gubbins*, 1985; *Jackson et al*., 2000] and time-averaged field studies suggest that these features may be truly long lived [e.g., *Gubbins and Kelly*; 1993; *Johnson and Constable*, 1995], analyses of CSHM suggest that these features are not truly persistent, but drift to and from preferred locations [e.g., *Bloxham*, 2002; *Dumberry and Finley*, 2006; *Korte and Holme*, 2010; *Amit et al*., 2010, 2011]. Given enough well dated high-resolution PSV records, CSHM will eventually be able to accurately resolve the evolution of nonaxisymmetric features. At present, however, the spatial and temporal resolution of CSHM are limited by the distribution and quality, including chronology, of available PSV data. As a result, our understanding of these significant geodynamo structures and their impact on PSV, even in the Holocene, remains poorly constrained.

[3] Paleomagnetic records preserved in deep-sea sediments have revolutionized our understanding of the longer-term variability of the geomagnetic field [*Opdyke and Channell*, 1996]. Variations in intensity, polarity reversals, and magnetic excursions have all been recovered from these archives [e.g., *Guyodo and Valet*, 1996; *Channell and Lehman*, 1997; *Lund et al*., 2006; *Laj and Channell*, 2007]. The recent focus on relative paleointensity is transforming our understanding of paleogeomagnetic change [*Tauxe*, 1993; *Valet*, 2003; *Tauxe and Yamazaki*, 2007; *Ziegler et al*., 2011], while providing an important new technique for high-resolution global stratigraphy [e.g., *Mazaud et al*., 1994, 2002; *Guyodo and Valet*, 1996, 1999; *Stoner et al*., 1995a, 2000, 2002; *Channell et al*., 2000, 2009; *Laj et al*., 2000, 2004]. In contrast, directions preserved in deep-sea sediment paleomagnetic records [e.g., *Lund and Keigwin*, 1994; *Lund et al*., 2005] are rarely considered in detail outside of reversals [e.g., *Channell and Lehman*, 1997; *Mazaud and Channell*, 1999; *Mazaud et al*., 2009] and excursions [e.g., *Lund et al*., 2005; *Channell*, 2006; *Laj et al*., 2006]. As a result, and largely owing to the fact that deep-sea sedimentation rates are usually not sufficiently high, locations like the northern North Atlantic that are optimal for constraining the behavior of nonaxisymmetric geomagnetic features [e.g., *Bloxham and Gubbins*, 1985; *Jackson et al*., 2000] are rarely utilized as archives of Holocene PSV.

[4] During Integrated Ocean Drilling Program (IODP) Expedition 303, drilling at Site U1305 (Lat.: 57°28.5 N, Long.: 48°31.8 W, water depth 3459 m; Figure 1 and Table 1) recovered an expanded version of a well-studied sediment sequence off southern Greenland in the Labrador Sea region of the northern North Atlantic Ocean [*Expedition 303 Scientists*, 2006]. Shipboard paleomagnetic measurements indicated that sediments from Site U1305 preserve directional variability consistent with Holocene PSV. Facilitated by the recent development of ultra-high resolution paleogeomagnetic records from surrounding regions [e.g., *St-Onge et al*., 2003; *Stoner et al*., 2007; *Genevey et al*., 2008], the recovery of undisturbed Holocene sediments at Site U1305 provides an unexpected opportunity to explore the full-vector Holocene paleomagnetic record of the northern North Atlantic.

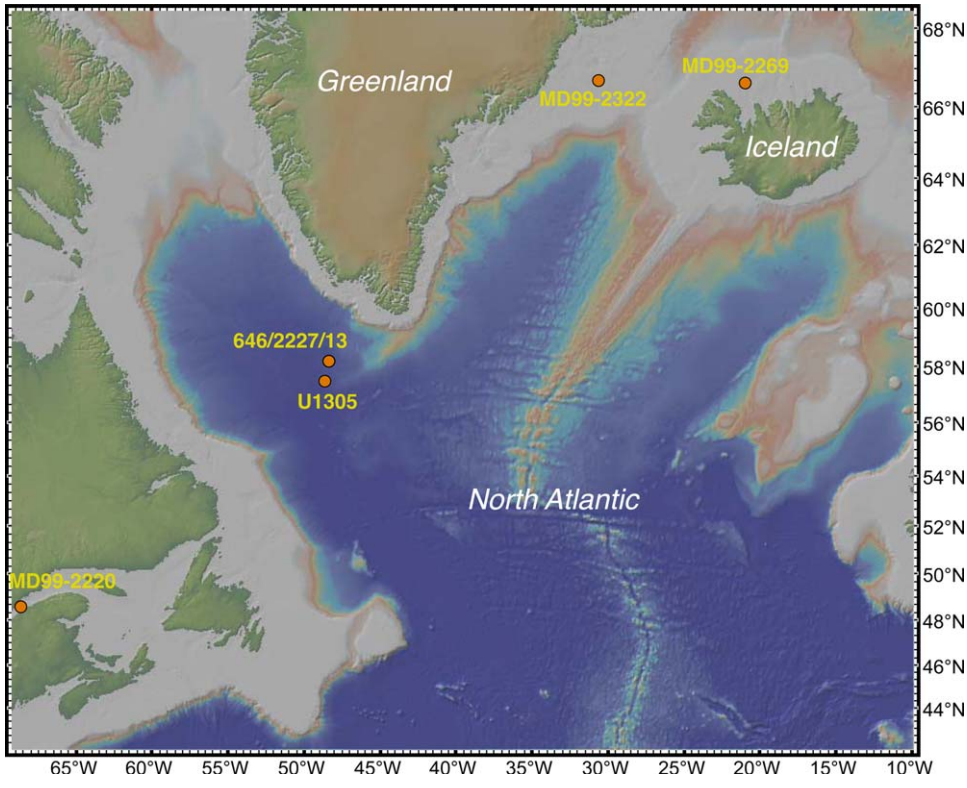

Figure 1. Map showing locations of sites studied or discussed in text. See Table 1 for latitudes, longitudes, and water depths. Base map provided by GeoMapApp [*Ryan et al*., 2009].

2. Regional Setting and Background

[5] Eirik Ridge, sometimes referred to as Eirik Drift, has been explored by the Ocean Drilling Program (ODP) Leg 105 [Site 646; *Srivastava et al*., 1987] and the Integrated Ocean Drilling Program (IODP) Exp. 303 [Sites U1305, U1306, and U1307; *Channell et al*., 2006] and several other coring cruises [e.g., *Hillaire-Marcel et al*., 1991; *Turon et al*., 1999]. The Pliocene-Quaternary depositional structure is fashioned by sediment redeposition as the Western Boundary Undercurrent (WBUC) sweeps around southern Greenland [*Johnson and Schneider*, 1969; *Srivastava et al*., 1987; *Hunter et al*., 2007]. IODP Site U1305 is located on the lee side of the southwestern extremity of the Eirik Ridge (Figure 1) where sediments accumulate rapidly during interglacials in response to a deepening of the WBUC [*Lucotte and Hillaire-Marcel*, 1994; *Hillaire-Marcel et al*., 1994a, *Hunter et al*., 2007]. Drilled 82 km south of previously lee side occupations (e.g., ODP Site 646; piston cores Hu90-013-013 and MD99-2227) (Figure 1 and Table 1), Site U1305 captures an expanded version of the previously observed lithologic pattern [e.g., *Expedition 303 Scientists*, 2006; *Hillaire-Marcel et al*., 2011; *Mazaud et al*., 2012]. Lithogenic sediments arrive at these sites from the erosive activity of the Greenland, Iceland, and Laurentide ice sheets and subsequent

Table 1. Sites Discussed in This Study

Site	Type	Latitude	Longitude	Water Depth (mbsl)
IODP Site U1305	IODP/APC	57 28.51′N	48 31.78′W	3458.8
Hu90-013-013	CSS Hudson Piston Core	58 12.59′N	48 22.40′W	3380.0
ODP Site 646	ODP/APC	58 12.56′N	48 22.15′W	3450.0
MD99-2227	IMAGES Calypso Core	58 12.64′N	48 22.32′W	3460.0
MD03–2265	IMAGES Calypso Core	57 26.56′N	48 36.60′W	3440.0
MD99-2269	IMAGES Calypso Core	66 37.53′N	20 51.16′W	365.0
MD99-2322	IMAGES Calypso Core	67 08.18′N	30 49.67′W	714.0
MD99-2220	IMAGES Calypso Core	48 38.32′N	68 37.93′W	320.0

redistribution by the WBUC, with rapidly deposited detrital layers commonly observed during times of ice sheet instability [*Hillaire-Marcel et al*., 1994a; *Stoner et al*., 1994, 1995b, 1996; *Evans et al*., 2007; *Hunter et al*., 2007; *Carlson et al*., 2008]. Biological productivity is highest during interglacials and the biogenic carbonate flux increases through the Holocene [*Hillaire-Marcel et al*., 1994a, 1994b]. The lithology reflects these environmental variations and ranges from silty clay with sand and little biogenic material during glacial and deglacial times, to homogenous nannofossil ooze with silty clay and common bioturbation during interglaciations [see, *Expedition 303 Scientists*, 2006]. As a result, sediments from the lee side of the Eirik Ridge have been used to reconstruct paleoceanographic [e.g., *Hillaire-Marcel et al*., 1994a, 1994b, 2001, 2011; *Hillaire-Marcel and Bilodeau*, 2000; *Fagel et al*., 1997, 2002, 2004; *Fagel and Hillaire-Marcel*, 2006; *Kleiven et al*., 2008; *Winsor et al*., 2012], ice sheet [e.g., *Hillaire-Marcel et al*., 1994a; *Stoner et al*., 1994, 1995b, 1996; *Evans et al*., 2007; *Carlson et al*., 2008; *de Vernal and Hillaire-Marcel*, 2008; *Kleiven et al*., 2008; *Colville et al*., 2011], and paleomagnetic [e.g., *Stoner et al*., 1995a, 1998; *Evans et al*., 2007; *Mazaud et al*., 2012] evolution over a range of time scales. The primary objective for drilling Site U1305 was to use IODP's advance piston coring (APC) technology to extend these high-quality records through the recovery of a complete uppermost Pliocene to Quaternary sediment section [*Expedition 303 Scientists*, 2006].

[6] The undisturbed recovery of an expanded postglacial Holocene section at Site U1305 [*Expedition 303 Scientists*, 2006, Site U1305] presented a significant and unexpected opportunity. Shipboard data and prior studies [e.g., *Hillaire-Marcel et al*., 1994a, 1994b; *Stoner et al*., 1994, 1995b, 1996; *Fagel et al*., 2004; *Evans et al*., 2007] suggest that the rapid accumulation of homogenous postglacial sediments would be ideal for paleomagnetic reconstructions. As a result of piston coring induced soft sediment deformation [e.g., *Turon et al*., 1999], earlier studies did not explicitly interpret the Holocene part of the record [*Stoner et al*., 1995a; *Evans et al*., 2007]. At Site U1305, a well-recovered Holocene is implied by preservation of horizontal structures including the Fe redox boundary at ~0.20 m composite depth (mcd) and the reproduction of shipboard physical and paleomagnetic properties from two overlapping Holes, Hole U1305B and Hole U1305C (see supporting information Figure fs01[1]) [*Expedition 303 Scientists*, 2006, Site U1305]. In contrast, data collected as part of *Stoner et al*. [1995a] (Hu90-013-013) and *Evans et al*., [2007] (MD99-2227) studies show that neither piston core yielded correlative nor clearly interpretable Holocene PSV records (see supporting information Figure fs01).

[7] U-channel samples from an optimal off-splice section were collected from the working halves of cores U1305A-1H, U1305C-1H, and U1305C-2H, measured and returned prior to the Expedition 303 Sampling Party, whereupon they were subsampled for other analyses. The focus of this study is the paleomagnetic record from 1305C-1H that captures an almost complete postglacial Holocene (ca. 8.2 ka) record from 0.05 to 5.1 mcd [*Expedition 303 Scientists*, 2006].

3. Magnetic Methods

[8] Magnetic remanence measurements before and after demagnetizations were performed using a 2G Enterprises superconducting rock magnetometer with inline alternating field (AF) coils designed to measure u-channel samples at the University of Florida. The natural remanent magnetization (NRM) of the u-channel samples were measured at 1 cm spacing before demagnetization, and after each of 12 AF demagnetization steps with peak fields from 10 to 100 mT (Figure 2). Though measured at a 1 cm interval, the response function of the magnetometer integrates ~4.5 cm (width at half-height) of stratigraphic depth [*Weeks et al*., 1993; *Guyodo et al*., 2002]. For each u-channel, anhysteretic remanent magnetization (ARM) was acquired in a peak AF of 100 mT and a 50 μT DC biasing field. ARM was also measured at a 1 cm interval before and after AF demagnetization at the same steps used for the NRM, up to peak AF of 60 mT (Figure 2). Isothermal remanent magnetization (IRM) was then acquired in a DC field of 0.3T and was measured and demagnetized using the same procedure as for the ARM (Figure 2).

[9] Volumetric magnetic susceptibility (κ) (Figure 2) was measured on u-channel samples at 1 cm spacing using a track built at the University of Florida with a Saffire Instruments SI2B magnetic susceptibility loop system that averages over 3 cm

[1]Additional supporting information may be found in the online version of this article.

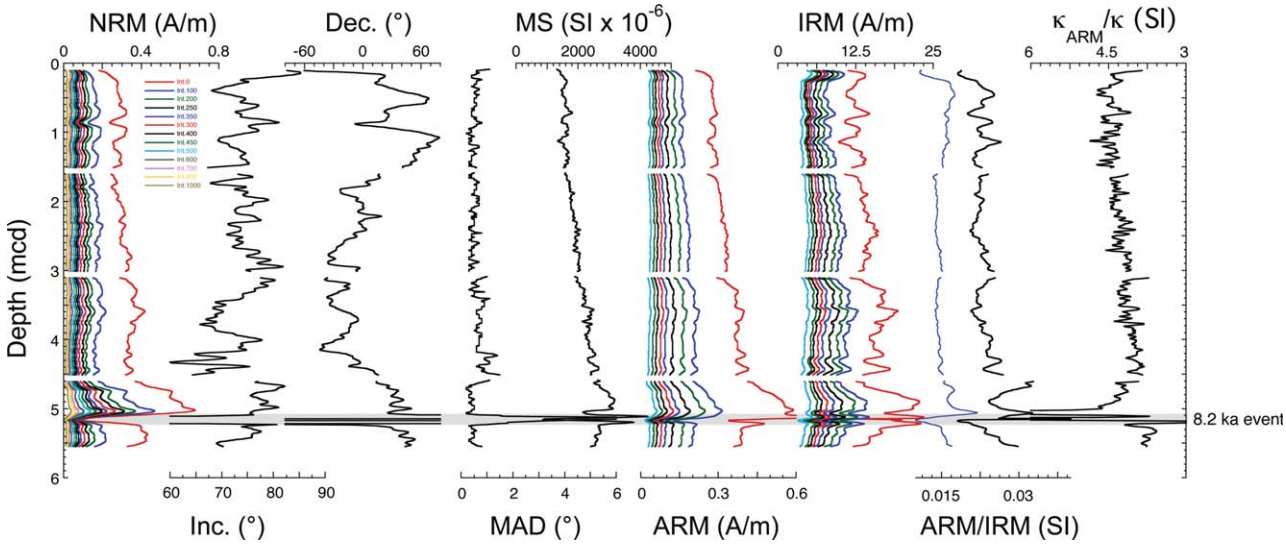

Figure 2. Down-core plot of paleomagnetic and rock magnetic data from Hole U1305C. From left to right: Intensity of the natural remanent magnetization (NRM) in A/m before and after progressive alternating field (AF) demagnetization. Characteristic remanent magnetization (ChRM) inclination and declination determined using principle component analysis (PCA) [*Kirschvink*, 1980] of measurements made after 10 AF demagnetization steps from 20 to 80 mT. Maximum angular deviation (MAD) values determined from the PCA analysis. Low-field volumetric magnetic susceptibility (κ). Intensity of the anhysteretic remanent magnetization (ARM) in A/m before and after alternating field (AF) demagnetization. Intensity of the isothermal remanent magnetization (IRM) in A/m before and after alternating field (AF) demagnetization. The ratio of ARM/IRM before and after 30 mT AF demagnetization. The ratio of anhysteretic susceptibility (κ_{ARM}) divided by κ.

[*Thomas et al*., 2003]. Normalizing ARM by the strength of the DC biasing field allows it to be expressed as an anhysteretic susceptibility (κ_{ARM}) and is used in concert with κ to produce a magnetic grain-size sensitive ratio κ_{ARM}/κ [*Banerjee et al*., 1981; *King et al*., 1982; *Stoner et al*., 1996] (Figures 2 and 3). Hysteresis parameters (M_{rs}, M_s, H_c, and H_{cr}) were acquired in a saturating field of 1000 mT on a Princeton Measurements Vibrating Sample Magnetometer at the Pacific Northwest Paleomagnetic Laboratory at Western Washington University.

4. Results

4.1. Natural and Laboratory Remanent Magnetizations

[10] Figure 2 illustrates the transition at ~4.5 mcd from the late deglacial, where large fluxes of terrigenous sediment are episodically delivered to the sea floor, to the postglacial Holocene where minimum ice conditions, increased productivity, and the general stability of the WBUC result in the consistent delivery of homogenous nannofossil ooze with silty clay [*Expedition 303 Scientists*, 2006]. The characteristic remanent magnetization (ChRM) directions (Figure 2) from u-channel NRM measurements were calculated by principal component analysis [*Kirschvink*, 1980] using 10 consecutive AF demagnetization steps with peak fields between 20 and 80 mT. Maximum angular deviation (MAD) associated with the ChRM calculation are less than 1.5° for the postglacial Holocene (Figure 2), indicating a consistently well-defined magnetization. ChRM inclinations vary around the geocentric axial dipole (GAD) inclination (~72°) for the site latitude (Figure 2). Because independent azimuthal control was not available for the uppermost cores, relative ChRM declinations were rotated to an entire core mean of zero (Figure 2). This assumption is reasonable and necessary, although only ~8000 years of geomagnetic behavior is averaged [e.g., *Merrill and McFadden*, 2003]. ChRM directions from the u-channel samples are consistent with shipboard derived paleomagnetic directions replicated from two holes at Site U1305 [*Expedition 303 Scientists*, 2006] (see supporting information Figure fs01).

[11] Hysteresis data derived from Site U1305 sediments are consistent with prior Eirik Ridge studies [*Stoner et al*., 1995a; *Evans et al*., 2007; *Kleiven et al*., 2008] and show that postglacial Holocene

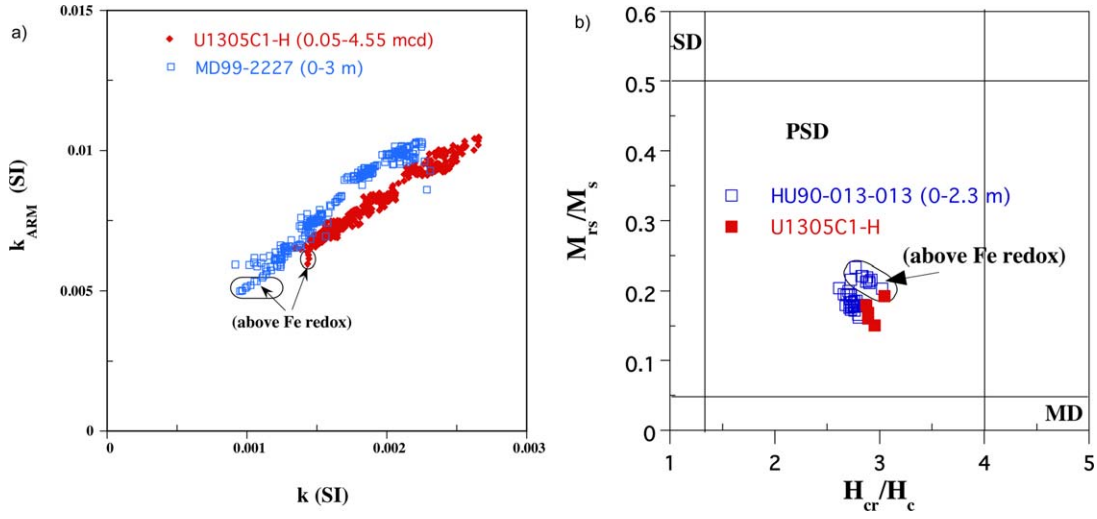

Figure 3. (a) Anhysteretic susceptibility (κ_{ARM}) plotted against susceptibility (κ) as a magnetic grain-size proxy after *Banerjee et al*. [1981] for the post-glacial sediments from the upper 4.5 mcd of Site U1305 compared with post-glacial sediments (upper 3 m) of Eirik Ridge core MD99-2227 [*Evans et al*., 2007]. (b) Magnetic hysteresis parameters (M_{rs}, saturation remanence; M_s, saturation magnetization; H_{cr}, coercivity of remanence; H_c, coercive force) for the post-glacial sediments from the upper 4.5 mcd of Site U1305 compared with those from post-glacial sediments (upper 2.3 m) of Eirik Ridge core Hu90-013-013 [*Stoner et al*., 1995b]. Single domain (SD), pseudo-singe domain (PSD), and multidomain (MD) fields are after *Day et al*. [1977]. Note: Cores MD99-2227 and Hu90-013-013 were collected from the same location. Sediments from above the Fe redox boundary (~the upper 20 cm) are indicated. 4 mT was added to the H_{cr} values from Site U1305 to correct for differences assumed to result from the data being acquired on different instruments at different times.

sediments fall within the pseudo-single domain (PSD) field on a *Day et al*. [1977] plot (Figure 3). Except for the oxidized upper ~20 cm, all samples fall on a single-domain to multidomain magnetite mixing line [*Dunlop and Carter-Stiglitz*, 2006]. On a *Banerjee et al*. [1981] plot (κ_{ARM} versus κ, Figure 3), postglacial Holocene sediments at Site U1305 display a linear trend indicating magnetic uniformity. Both hysteresis and κ_{ARM}/κ data indicate that postglacial Holocene sediments at Site U1305 are similar to, but magnetically coarser (Figure 3) than those observed from prior lee side occupations 82 km further to the north (e.g., ODP Site 646; cores Hu90-013-013 and MD99-2227) [*Stoner et al*., 1995a; *Evans et al*., 2007] (Figure 1). The strong, low-coercivity magnetization at Site U1305 is consistent with magnetite being the primary remanence carrier, as found in other Erik Ridge studies [e.g., *Stoner et al*., 1995a, 1995b; *Evans et al*., 2007; *Kawamura et al*., 2012; *Mazaud et al*., 2012]. While the higher accumulation rates and slightly coarser magnetic grain sizes at the more proximal Site U1305 location further implicate the WBUC in the deposition of these sediments.

[12] The postglacial Holocene sediments above 4.5 mcd at Site U1305 fall within the criteria of *King et al*. [1983] and *Tauxe* [1993] for sediments likely to provide reliable relative paleointensity (RPI) estimates (Figures 2 and 3). NRM, ARM, IRM, and κ all vary by less than a factor of two (Figure 2), well within the order of magnitude advocated by *Tauxe* [1993] for variations in magnetic mineral concentrations. Magnetic grain size, indicated by κ_{ARM}/κ and ARM/IRM at Site U1305 (Figures 2 and 3), and hysteresis ratios from this and previous regional studies [*Stoner et al*., 1995b, 1996; *Evans et al*., 2007; *Kleiven et al*., 2008], show only minor down-core variations. NRM normalized by ARM and IRM for all demagnetization steps between 10 and 60 mT with mean ratios and slope values of the best-fit lines calculated using the UPmag software [*Xuan and Channell*, 2009] are shown in Figure 4. Similar to many North Atlantic normalized remanence records [e.g., *Channell et al*., 1997; *Stoner et al*., 2000; *Evans et al*., 2007], NRM/ARM increases with increasing peak AF, while NRM/IRM decreases (Figure 4), indicating that neither is a perfect coercivity-match to the NRM, although the

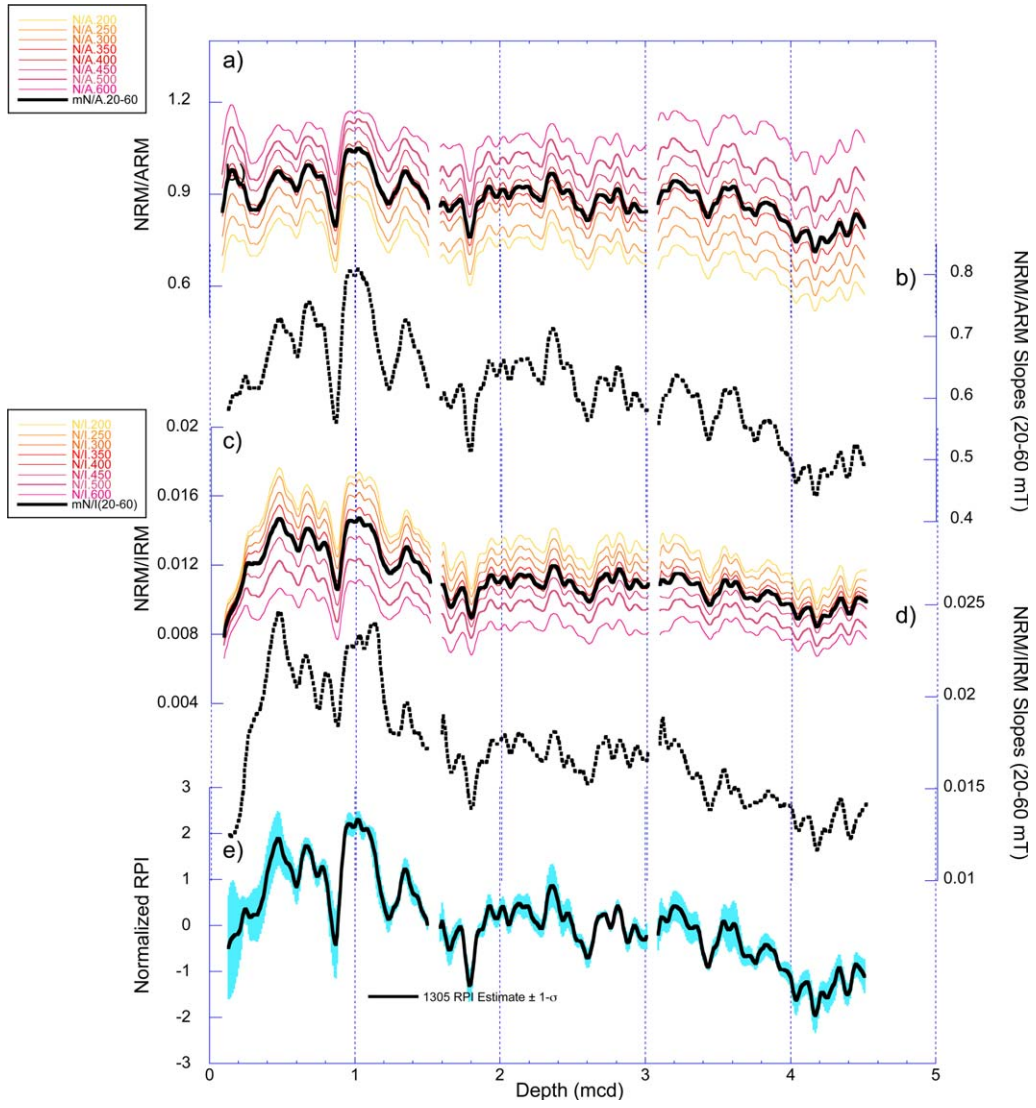

Figure 4. Comparison between different NRM normalization techniques. (a) NRM/ARM for all AF demagnetization steps from 10 to 60 mT and their mean (bold line). (b) NRM/ARM slope over the 10–60 mT AF demagnetization window. (c) NRM/IRM for all AF demagnetization steps from 10 to 60 mT and their mean (bold line). (d) NRM/IRM slope over 10–60 mT AF demagnetization window. (e) The average of all four normalized remanence estimates after scaling each record to a mean of zero and normalized by their standard deviation. This represents our preferred relative paleointensity proxy and its ±1 standard deviation uncertainty (blue envelope).

means and slopes of the two RPI estimates are similar (Figure 4). To check if the normalized remanence records are independent from and therefore not contaminated by their normalizers, we calculate the squared wavelet coherence between the mean NRM/ARM and ARM, and between the mean NRM/IRM and IRM. The calculation is performed both before and after the records are placed on an age model. Squared wavelet coherence measures the similarity of the cross-wavelet transforms of two time series in the time-frequency domain. Compared with traditional coherence analysis methods [e.g., *Tauxe and Wu*, 1990; *Tauxe*, 1993], which identify frequency bands within which the two time series are covarying, the squared wavelet coherence is used to identify both the frequency bands and time intervals within which the two time series are covarying significantly [e.g., *Torrence and Webster*, 1999; *Xuan and Channell*, 2008]. Little significant coherence in depth or time was observed between the normalized remanence and either normalizer (see supporting information, Figure fs02) suggesting that these sediments provide reliable RPI

estimates. The RPI proxies are similar (Figure 4), although NRM/IRM implies higher intensities for the upper 1.5 mcd and a rapid intensity drop over the upper 0.25 mcd, not observed in the NRM/ARM records. Because the variance within the normalized remanence values are similar and coercivity of NRM falls between that of ARM and IRM, we average the means and the slopes of NRM/ARM and NRM/IRM to estimate postglacial relative paleointensity and its uncertainty at Site U1305 (Figure 4).

4.2. Radiocarbon Chronology for Site U1305

[13] The most recent rapidly deposited detrital layer, observed between 5.11 and 5.22 mcd (U1305C-1H-4, 56–67 cm) [*Expedition 303 Scientists*, 2006] marks the base of the studied section. This visually identifiable layer is unique when compared with other rapidly deposited detrital layers [e.g., *Stoner et al*., 1996; *Evans et al*., 2007; *Kleiven et al*., 2008] as it is associated with fine magnetic grain sizes and low concentrations intercalated within a magnetically coarser, higher concentration interval (Figure 2). *Kleiven et al*. [2008] dated this layer in nearby core MD03–2665 (Figure 1 and Table 1) at ~ 8.3 Cal kyrs B.P. and attributed it to the outburst flood of glacial Lake Agassiz [*Barber et al*., 1999; *Lajeunesse and St-Onge*, 2008]. The discharge of fresh water associated with this event is thought to have been responsible for the "8.2" climate event [*Alley et al*., 1997; *Kleiven et al*., 2008] dated at 8236 ± 47 cal yrs BP in the Greenland NGRIP Ice Core [*Rasmussen et al*., 2006]. Sedimentation rates and the age model above this layer are constrained by 17 calibrated radiocarbon dates derived from mixed planktonic foraminifera picked from the >125 μm fraction (Figure 5 and Table 2). Radiocarbon analyses were performed at the UC Irvine Keck AMS facility. Radiocarbon dates were converted to calendar ages using CALIB 6.02 INTCAL09 [*Reimer et al*., 2009] with a standard ~400 yr marine reservoir correction (Table 2). These dates describe sedimentation rates that vary from ~35 to 90 cm/kyr for the upper 4.5 mcd with higher sedimentation rates below. A few dates fall off this general trend (Figure 5 and Table 2). An age reversal is observed for the oldest two dates, when considered along with the observation of the "8.2" event, implies exceptionally rapid sedimentation (>2 m/kyr) below ~4.5 mcd. A 2-σ age overlap is observed between dates at 2.85 and 3.10 mcd implying rapid sediment accumulation in this interval, with much lower rates above (Figure 5). At present, however, there is little lithologic evidence to support this and therefore our preferred age model is constrained by 8.2 ka event, prescribed with an age of 8250 cal yr BP at 5.15 mcd, with a linear interpolated fit to all but two of the dates above (Figure 5 and Table 2).

4.3. Regional PSV and RPI Comparisons

[14] Three Marion Dufresne II (MD) cores obtained from ultra-high resolution (>100 cm/kyr) continental margin sediments (Figure 1 and Table 1) help define the Holocene paleomagnetic record of the Labrador Sea region of the northern North Atlantic Ocean. Core MD99-2269 collected from Húnaflói on the north Iceland shelf and core MD99-2322 collected from the deepest part of the Kangerlussuaq Trough on the southeast Greenland shelf [*Stoner et al*., 2007] are located northeast of Site U1305 (Figure 1). The declination and inclination records from both cores are combined into a single composite PSV record based on correlation between the two sites [*Stoner et al*., 2007] (Figure 6). The Greenland/Iceland PSV composite averages the PSV records from these two MD cores during periods of overlap, while using the best available record to fill gaps caused by sediment deformation and section breaks. An initial age model for these cores was developed using 25 radiocarbon dates from core MD99-2269 and 19 from core MD99-2322 combined into a single age to depth relationship [*Stoner et al*., 2007]. To account for radiocarbon reservoir age uncertainties in the Nordic Seas [e.g., *Eiriksson et al*., 2004], terrestrial ages of seven crypto-tephras and 1 discrete tephra layer (Saksunarvatn) in core MD99-2269 [*Kristjansdottir et al*., 2007] were used to further adjust the *Stoner et al*. [2007] age model. This results in a chronology up to 250 yrs younger (mean ~ 130 yrs, median ~ 90 yrs) than previously reported [*Stoner et al*., 2007] (Figure 6b). The Greenland/Iceland PSV composite has a nominal 5 yr resolution, although additional smoothing due to stacking, sedimentation rate changes, and the response function of the u-channel magnetometer are not taken into account. High mean sedimentation rates of ~200 cm/kyr in both cores and minimal mixing depth of 5–15 cm (based on cryptotephra distributions, G. Kristjansdottir, personal communication, 2008 and A. Jennings, personal communication, 2010) implies that the age of these sediments should provide a reasonable estimate for the age of the magnetization. This is supported by agreement between the

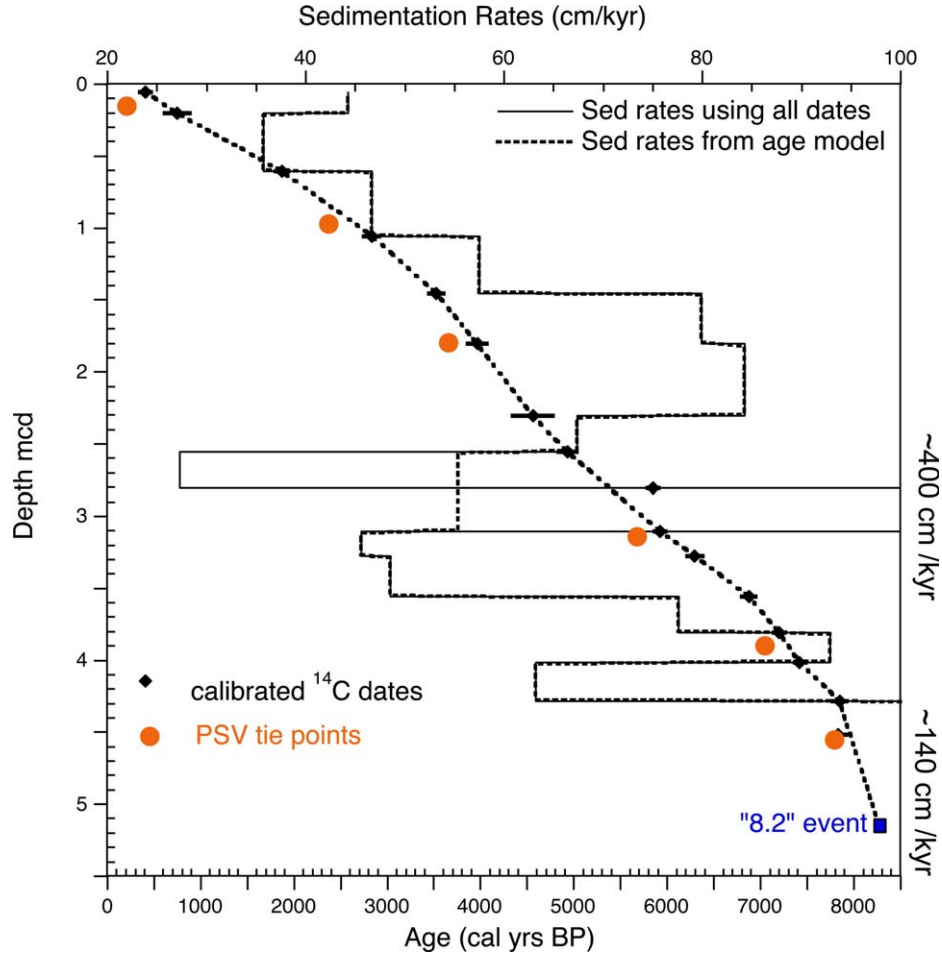

Figure 5. Age models and sedimentation rates for IODP Site U1305. (a) The age to depth relationship for Site U1305 is based on 17 calibrated radiocarbon dates derived from mixed planktonic foraminifera (Table 2) and the identification of the "8.2 event" on the Eirik Ridge [e.g., *Kleiven et al*., 2008]. Dates were calibrated with Calib 6.02 using INTCAL09 [*Reimer et al*., 2009] assuming a standard ~400 yr marine reservoir correction (Table 2). Error bars reflect their 2-σ calibrated age. Our preferred age model uses a prescribed age of 8250 cal yr BP at 5.15 mcd for the "8.2 event" with a linear interpolated fit to all but two of the dates above (Figure 5 and Table 2). Estimated sedimentation rates are shown for our preferred age model (stippled black line) and for all dates (light gray).

Greenland/Iceland PSV composite and CSHM (ARCH3k_cst.1) predictions [*Korte et al*., 2009] (Figure 6). It should be noted that there is less agreement between Greenland/Iceland PSV composite and model predictions made with less constrained data sets [*Korte and Constable*, 2011; *Korte et al*., 2011]. ARCH3k_cst.1 is derived exclusively from archeomagnetic data that passes quality criteria [*Donadini et al*., 2009], suggesting that data quality (including chronology) may be more important than data completeness for the accuracy of CSHM predictions in reasonably well-constrained locations.

[15] Another existing ultra-high resolution PSV record to the southwest of Site U1305 is core MD99-2220 from the St Lawrence estuary (Figure 1) [*St-Onge et al*., 2003]. The fidelity of this paleomagnetic record is supported by recent PSV and RPI stacks from the same region [*Barletta et al*., 2010]. The age model for core MD99-2220 is based on six calibrated AMS radiocarbon dates augmented by an additional eight dates transferred through lithologic correlation from nearby core MD99-2221 [*St-Onge et al*., 2003]. The high mean sedimentation rate of ~150 cm/kyr and the minimal mixed layer thickness, estimated at 5–10 cm based on ^{210}Pb analysis [*St-Onge et al*., 2003], implies that the age of the sediment is a close estimate for the age of the magnetization. Assuming that the control of the geomagnetic field on the production of cosmogenic nuclides [e.g., *Elsasser*

Table 2. Radiocarbon Dates from Site U1305

Site U1305	Radiocarbon Dates	Calibrated Radiocarbon Ages		
		Min 2σ	Med. Prob.	Max 2σ
Depth (mcd)	Reported Age ^{14}C years BP	Cal yrs BP	Cal yrs BP	Cal yrs BP
0.055	760 ± 20	320	409	465
0.205	1200 ± 60	650	748	884
0.605	2260 ± 15	1806	1867	1932
1.055	3070 ± 20	2760	2832	2913
1.455	3630 ± 15	3453	3527	3601
1.805	3970 ± 20	3881	3965	4063
2.305	4400 ± 50	4410	4558	4723
2.555	4710 ± 25	4847	4929	5023
2.805	5460 ± 20	5751	5846	5901
3.105[a]	5540 ± 20	5875	5922	5982
3.275	5880 ± 20	6246	6295	6375
3.555	6395 ± 20	6785	6872	6947
3.805	6655 ± 20	7141	7194	7249
4.005	6905 ± 20	7361	7420	7477
4.285	7375 ± 20	7777	7847	7918
4.515[a]	7360 ± 25	7748	7829	7913

[a]Dates not used in age model shown in Figure 5.

et al., 1956] holds even at centennial timescales, *St-Onge et al*. [2003] took the additional step of correlating the RPI from core MD99-2220 to the well-dated record of radiocarbon production [*Stuiver et al*., 1998]. Age adjustments of no more than 200 yrs, well within chronological uncertainty, were required to maximize this correlation. This supports the contention that the geomagnetic shielding model for cosmogenic nuclide production extends to submillennial time scales [*St-Onge et al*., 2003] and that the age of magnetization in core MD99-2220 is close to the age of the sediment.

[16] Using the radiocarbon-based age model in Figure 5, inclination and declination patterns for Site U1305 are shown in Figure 7. Comparisons, with ultra-high resolution PSV records from the Greenland/Iceland composite and the St. Lawrence Estuary, and the ARCH3k_cst.1 CSHM predictions, show that Site U1305 preserves similar features, but at consistently older ages. Using a limited number of tie points (6) and linear interpolation, the ages of PSV features can be adjusted using the Analyseries program [*Paillard et al*., 1996] to obtain a higher degree of correlation (Figure 8). The tie points used to adjust Site U1305 to the Greenland/Iceland composite are shown in Figures 7 and 8. Correlation coefficients (r) between Site U1305 and the Greenland/Iceland composite record obtained after tuning (Figure 8) are high ($r = 0.75$ for declination and $r = 0.343$ for inclination), while those to core MD99-2220 are lower ($r = 0.505$ for declination and $r = 0.33$ for inclination). Higher correlation coefficients could be obtained using more tie points. Lower correlation coefficients are observed to either PSV record with Site U1305 on its radiocarbon age model (to the Greenland/Iceland composite $r = 0.616$ for declination and $r = -0.092$ for inclination; to core MD99-2220 $r = -0.12$ for declination and $r = 0.134$ for inclination) as in Figure 7.

[17] Comparisons between the Site U1305 RPI record on the tuned chronology with the European archeomagnetic intensity compilation [*Genevey et al*., 2008], intensity predictions for the northern North Atlantic from ARCH3k_cst.1 CSHM [*Korte et al*., 2009], and St. Lawrence Estuary core MD99-2220 RPI [*St-Onge et al*., 2003] are shown in Figure 9. When compared with the European archeomagnetic intensity record, again correlation coefficients are lower ($r = 0.64$) with Site U1305 RPI on a radiocarbon-based age model and higher ($r = 0.77$) after PSV tuning as in Figures 8 and 9. Similarities with the ARCH3k_cst.1 intensity predictions for Site U1305 suggest that differences between European and North Atlantic records reflect regional geomagnetic differences. Comparisons to St. Lawrence Estuary RPI record show that it is less similar (Figure 9) with lower correlation coefficients ($r = 0.61$). Regional studies suggest that these differences grow as one moves west over North American [e.g., *King et al*., 1983; *Lund and Banerjee*, 1985; *Lund and Schwartz*, 1999; *Brachfeld and Banerjee*, 2000; *St-Onge et al*., 2003; *Genevey et al*., 2008; *Barletta et al*., 2010].

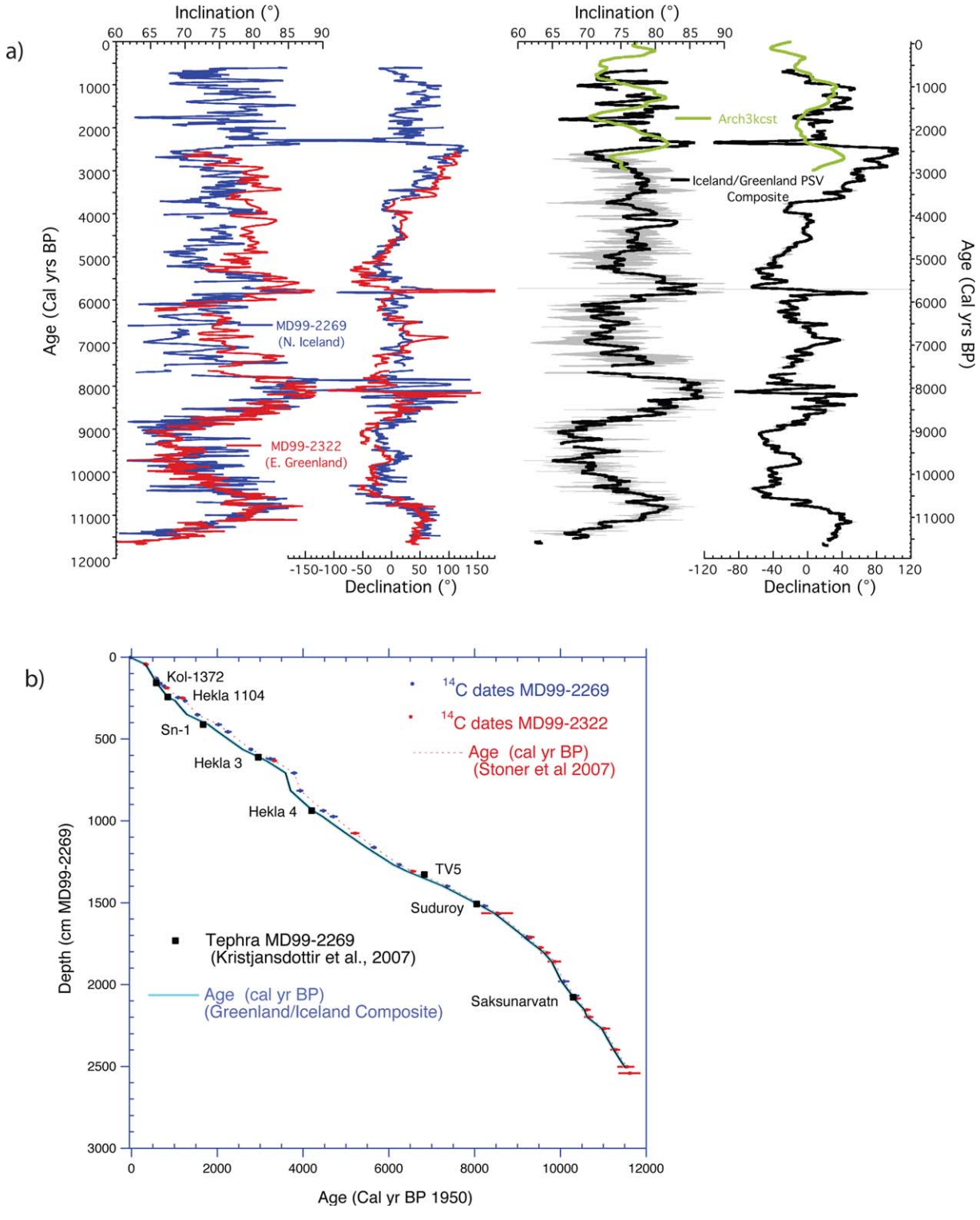

Figure 6. Development of the Greenland/Iceland PSV composite. (a) From left to right, the inclination and declination records from core MD99-2269 (blue) and core MD99-2322 (red) [*Stoner et al*., 2007] combined into 25 yr running mean inclination and declination records (black) with their associated ±1 standard deviations (gray). Site predictions from CSHM (ARCH3k_cst.1) are shown in green [*Korte et al*., 2009]. (b) The age model for PSV composite builds upon that of *Stoner et al*. [2007] where 25 calibrated radiocarbon dates from core MD99-2269 (blue circles) and 19 calibrated radiocarbon dates (red squares) from core MD99-2322 were combined into a single age to depth relationship. Terrestrial ages of 7 crypto-tephras and 1 discrete tephra layer (Saksunarvatn) as identified by *Kristjansdottir et al*. [2007] in core MD99-2269 (black squares) were used to account for radiocarbon reservoir age uncertainties in the *Stoner et al*. [2007] age model (blue line).

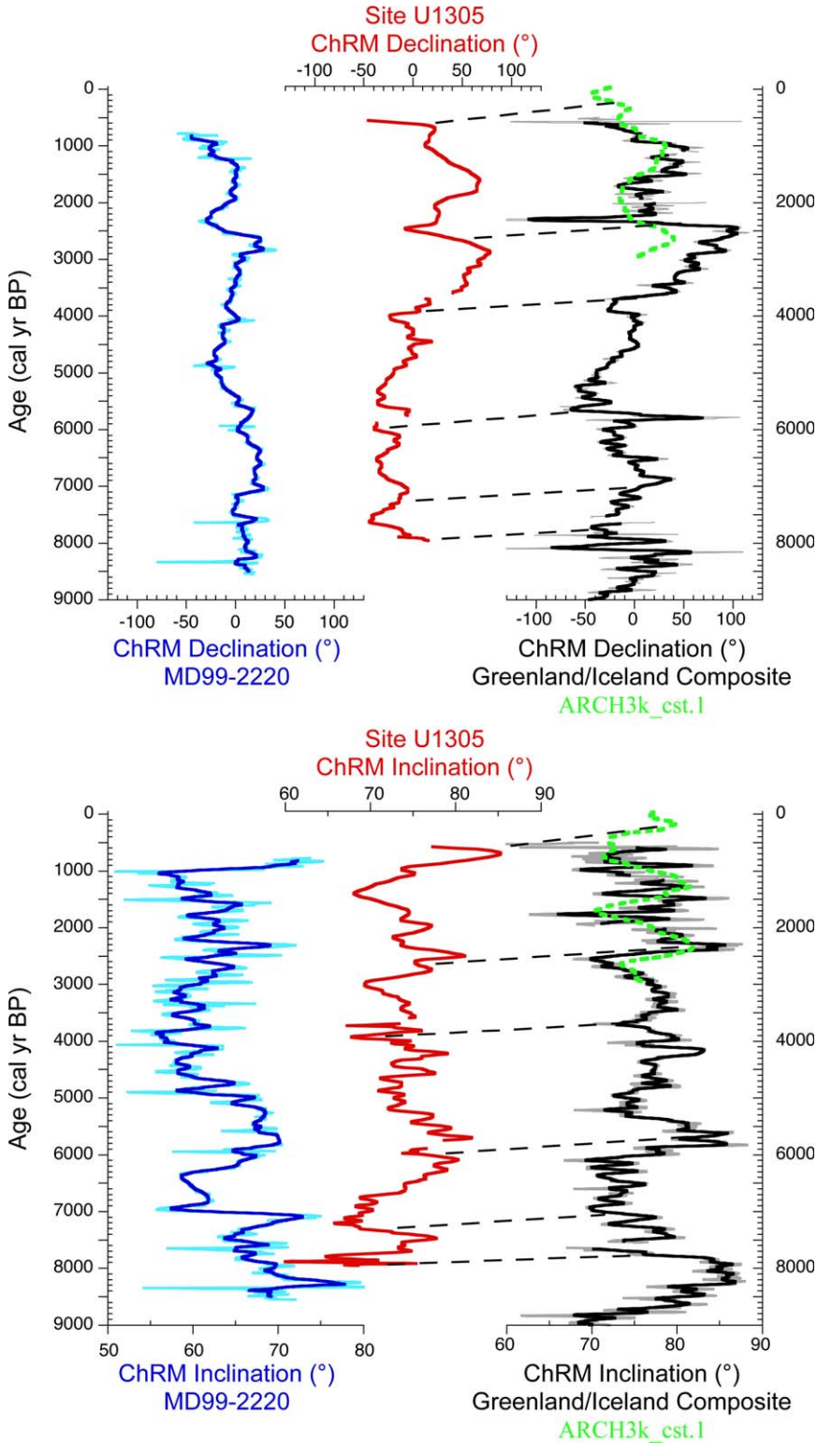

Figure 7. Comparison of the Site U1305 PSV record with ultrahigh resolution regional PSV records on their independent chronologies. (a) ChRM declinations from left to right, core MD99-2220 (blue) [*St-Onge et al*., 2003], the upper 4.5 mcd of Site U1305 (red) on the age model developed in Figures 5, the Greenland/Iceland PSV composite (black) developed in Figure 6 overlain with the ARCH3k_cst.1 predictions (green stippled) [*Korte et al*., 2009]. (b) ChRM inclinations from left to right, core MD99-2220 (blue), the upper 4.5 mcd of Site U1305 (red) on the age model developed in Figure 5, the Greenland/Iceland PSV composite (black) developed in Figure 6 overlain with the ARCH3k_cst.1 predictions (green stippled) [*Korte et al*., 2009]. Tie points (Table 3) used to adjust the Site U1305 PSV record in Figure 8 are shown as dashed lines. For locations see Figure 1 and Table 1.

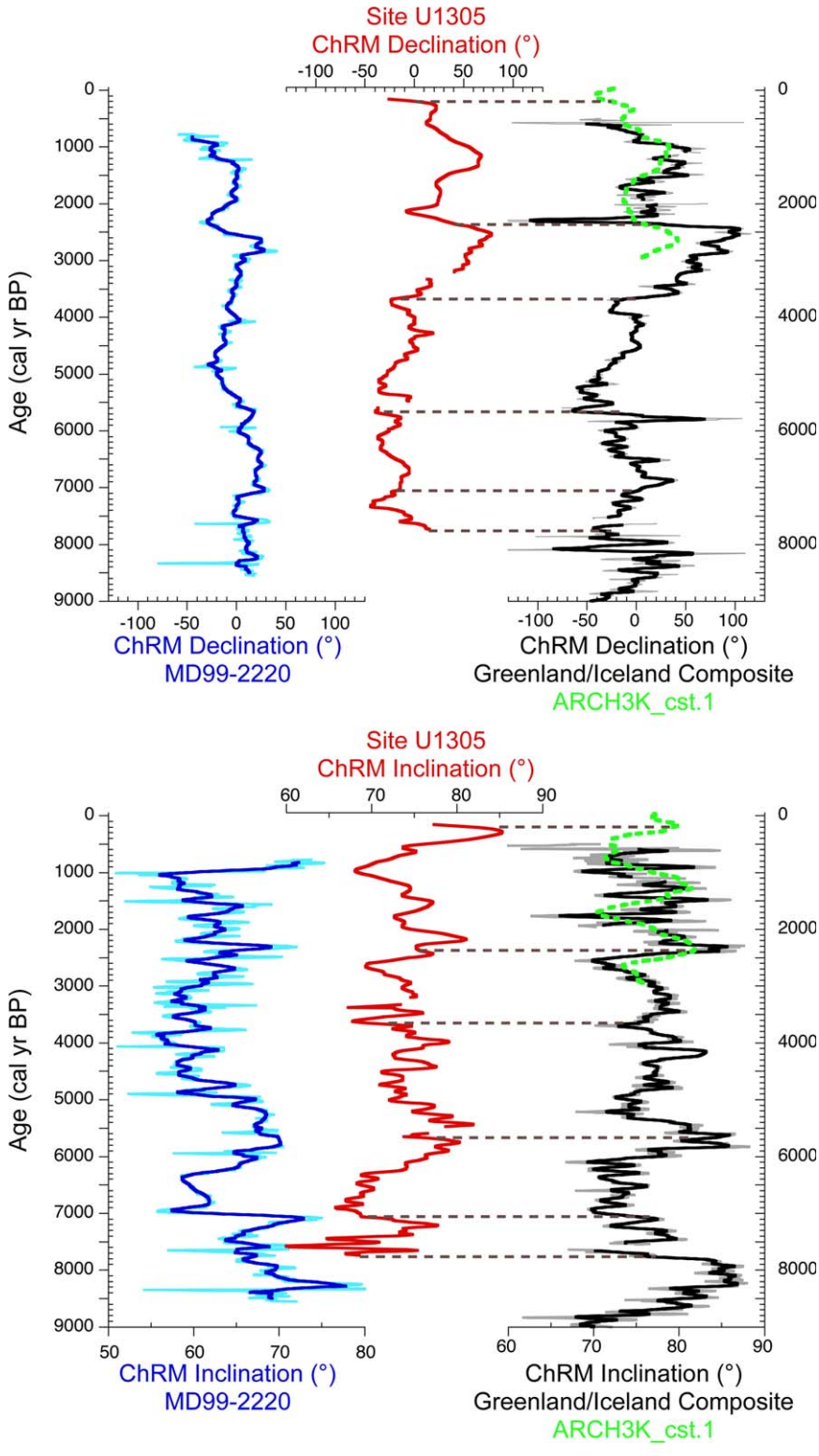

Figure 8. Comparison of the Site U1305 PSV record with ultrahigh resolution regional PSV records after tuning. (a) ChRM declinations from left to right, core MD99-2220 (blue) [*St-Onge et al*., 2003], the upper 4.5 mcd of Site U1305 (red) tuned to the Greenland/Iceland PSV composite, the Greenland/Iceland PSV composite (black) developed in Figure 6 overlain with the ARCH3k_cst.1 predictions (green stippled) [*Korte et al*., 2009]. (b) From left to right: ChRM inclinations from left to right, core MD99-2220 (blue), the upper 4.5 mcd of Site U1305 (red) tuned to the Greenland/Iceland PSV composite, the Greenland/Iceland PSV composite (black) developed in Figure 6 overlain with the ARCH3k_cst.1 predictions (green stippled) [*Korte et al*., 2009]. Tie points (Table 3) used to adjust the Site U1305 PSV record are shown as dashed lines. For locations see Figure 1 and Table 1.

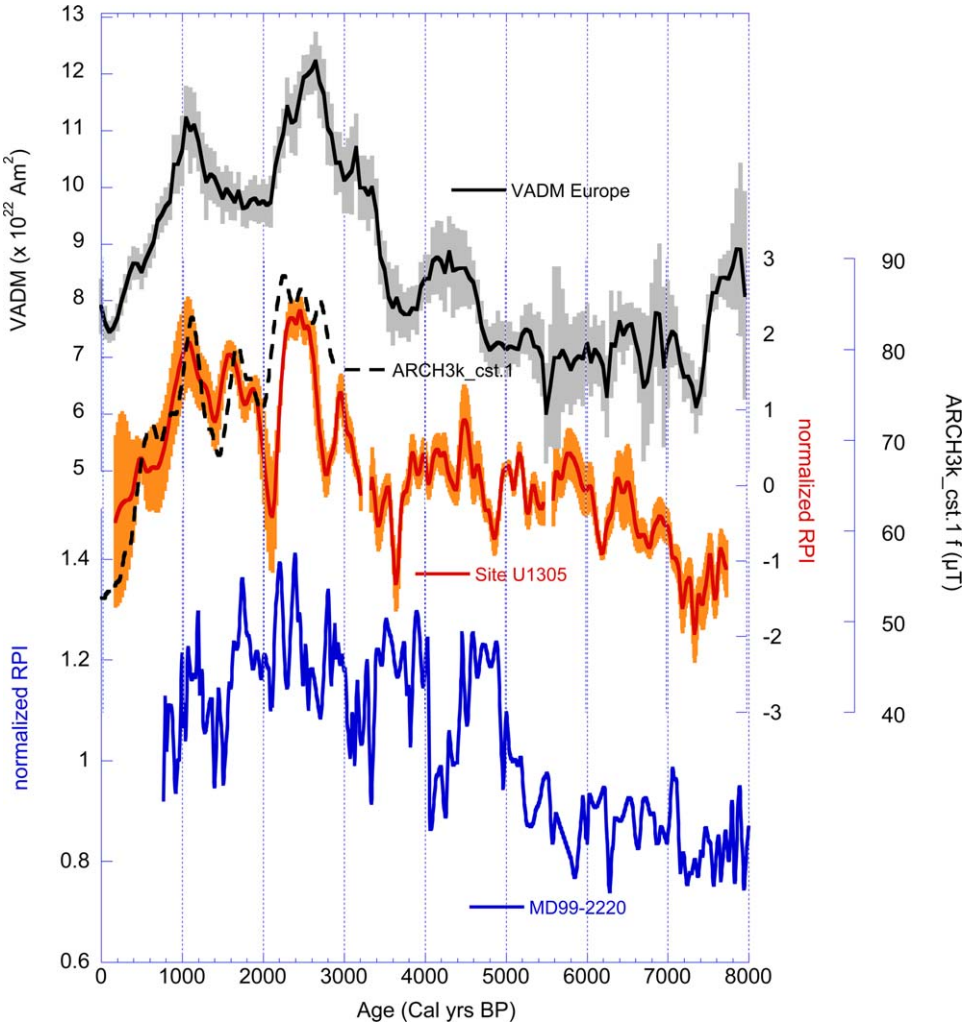

Figure 9. Paleointensity comparison across the North Atlantic. From top to bottom, the European archeomagnetic intensity compilation (black) [*Genevey et al*., 2008], RPI estimate for Site U1305 (red) as developed in Figure 4 on the tuned chronology in Figure 8, overlain by ARCH3k_cst.1 intensity predictions for the northern North Atlantic (black stippled) [*Korte et al*., 2009], and the RPI record from St Lawrence Estuary core MD99-2220 (blue) record [*St-Onge et al*., 2003].

4.4. Age of the Magnetization

[18] It is generally assumed that sediments acquire their remanent magnetization not at deposition, but at depth through a mechanism termed post-depositional remanent magnetization (pDRM) [*Irving and Major*, 1964; *deMenocal et al*., 1990; *Channell and Guyodo*, 2004; *Suganuma et al*., 2010]. This results in the age of the magnetization being younger than the age of the sediment as determined by the radiocarbon dated planktonic foraminifera. Assuming that the age of magnetization in this region is best defined by robustly dated (as described above) PSV records with the highest sedimentation rates (>200 cm/kyr), where the time lag between magnetization acquisition and sediment deposition is minimized. Allows us to estimate and correct for temporal offsets (from pDRM or any other reason) to derive a reasonable age for the magnetization at Site U1305. The age depth relationship that results from the six tie points (Table 3) is shown in Figure 5 (red dots).

Table 3. Tie Points

	Age		Offset	
Depth mcd (m)	Radiocarbon Age model (cal yrs BP)	(Green/Ice) (cal yrs BP)	Age (yrs)	Depth (cm)
0.15	612	211	401	15
0.97	2650	2368	282	13
1.8	3959	3655	304	24
3.14	5999	5674	325	17
3.91	7296	7046	250	21
4.5	7960	7790	170	25

The differences between the paleomagnetically tuned age model and the calibrated radiocarbon age model at the tie points is on average -289 ± 77 yrs at the same depth and 20 ± 5 cm at the same age (Figure 5 and Table 3). This ~20 cm depth offset is consistent with other pDRM estimates [*deMenocal et al*., 1990; *Channell and Guyodo*, 2004; *Suganuma et al*., 2010]. Any unrecognized radiocarbon reservoir ages (ΔR) greater than the standard marine reservoir correction [e.g., *Tisnerat-Laborde et al*., 2010] would affect these estimates. However, on the timescale of interest here, the subarctic North Atlantic during the postglacial Holocene is thought to reflect global surface ocean [*Broecker et al*., 1985; *Bard*, 1988] or slightly negative ΔR [*Reimer et al*., 2002] values, justifying the use of a standard marine reservoir correction [e.g., *Hillaire-Marcel et al*., 2001, 2007; *Fagel et al*., 2004; *Carlson et al*., 2008; *Kleiven et al*., 2008].

5. Discussion

5.1. Paleogeomagnetic Record of the Northern North Atlantic

[19] Transforming the PSV records (Figure 8) into virtual geomagnetic poles (VGP) by mapping a geocentric dipole that would cause the observed PSV record provides a way to visualize PSV while taking site location into account (Figures 10 and 11). Even though the records are derived from cores collected from locations with different deposition rates and sediment environments, VGP latitudes and longitudes derived from Site U1305 and the Greenland/Iceland composite are similar, supporting the interpretation of a regional geomagnetic origin of the common signal. Even the large amplitude change centered at ~2500 Cal years BP, where VGP latitudes deviate more than 40° from a geocentric axial dipole (GAD) is reproduced (Figure 10). This large deviation in VGP latitude is a result of the large eastward deviation in declination at this time. It should be noted that VGP latitudes are sensitive to declination and therefore, to the zero-mean declination assumption. Additional replication from archives with azimuthal control should be sought to confirm these observations. VGP latitudes from core MD99-2220 do not show such a large departure from GAD at ~2500 cal yrs BP, but rather a series of lower latitude VGP intervals every few thousand years (Figure 10). The differences between this North American and the North Atlantic records are even more apparent when comparing VGP longitudes (Figure 10). Core MD99-2220 is separated by ~1800 km from Site U1305, not much farther than Greenland/Iceland composite sites (~1600 km), yet differences in the records imply that North America and the northern North Atlantic have distinct geomagnetic behaviors, with the northern North Atlantic appearing more European in character [e.g., *Thompson and Barraclough*, 1982; *Lund*, 1996]. Comparisons between paleointensity records (Figure 9) support this contention. The RPI record from Site U1305 shows substantial similarity with European archeomagnetic intensity record ($r = 0.77$) and less with St. Lawrence Estuary ($r = 0.61$) or any other North American RPI record [e.g., *King et al*., 1983; *Lund and Banerjee*, 1985; *Brachfeld and Banerjee*, 2000; *Barletta et al*., 2010].

[20] Comparisons between northern North Atlantic VGPs and north geomagnetic pole reconstructions, either from VGP [*Nilsson et al*., 2011] or CSHM [*Korte et al*., 2005, 2011], show substantial similarity (for clarity only the *Nilsson et al*. [2011] reconstruction is shown in Figures 11 and 12). Considering that North Atlantic data were not included in the *Nilsson et al*. [2010, 2011] reconstructions, the similarities are intriguing and suggest that the northern North Atlantic is particularly sensitive to the global signal though with much greater amplitude (Figure 11).

[21] Observations of a geomagnetic field that deviates substantially from a GAD at around 2500 cal yrs BP (Figures 10 and 12) have been recognized elsewhere. Results from lavas from western North America [*Hagstrum and Champion*, 2002] and Hawaii [*Mankinen and Champion*, 1993; *Herrero-Bervera and Valet*, 2007] display shallow inclinations and far sided VGP locations, while European inclinations are steep with VGP latitudes almost 30° near sided [*Thompson and Turner*, 1979, *Gallet et al*., 2002; *Snowball et al*., 2007, *Haltia-Hovi et al*., 2010]. Even global reconstructions [*Nilsson et al*., 2010, 2011] show substantial deviations from a GAD field at that time (Figure 11). Excursional directions from around this time have even been reported [e.g., *Raspopov et al*., 2003, *Dergachev et al*., 2004], with key records coming from Georgian archeomagnetic data, and Baltic and Barents Seas sediments. Though evidence for a magnetic excursion at this time is tenuous, the VGP positions estimated using both Site U1305 data and the Greenland/Iceland composite deviate by more than 40° from GAD (Figures 10–12), and therefore, could be classified as excursional [*Barbetti and McElhinny*, 1972]. Observations of high-amplitude PSV in the North Atlantic region are reinforced by excursional directions from Icelandic

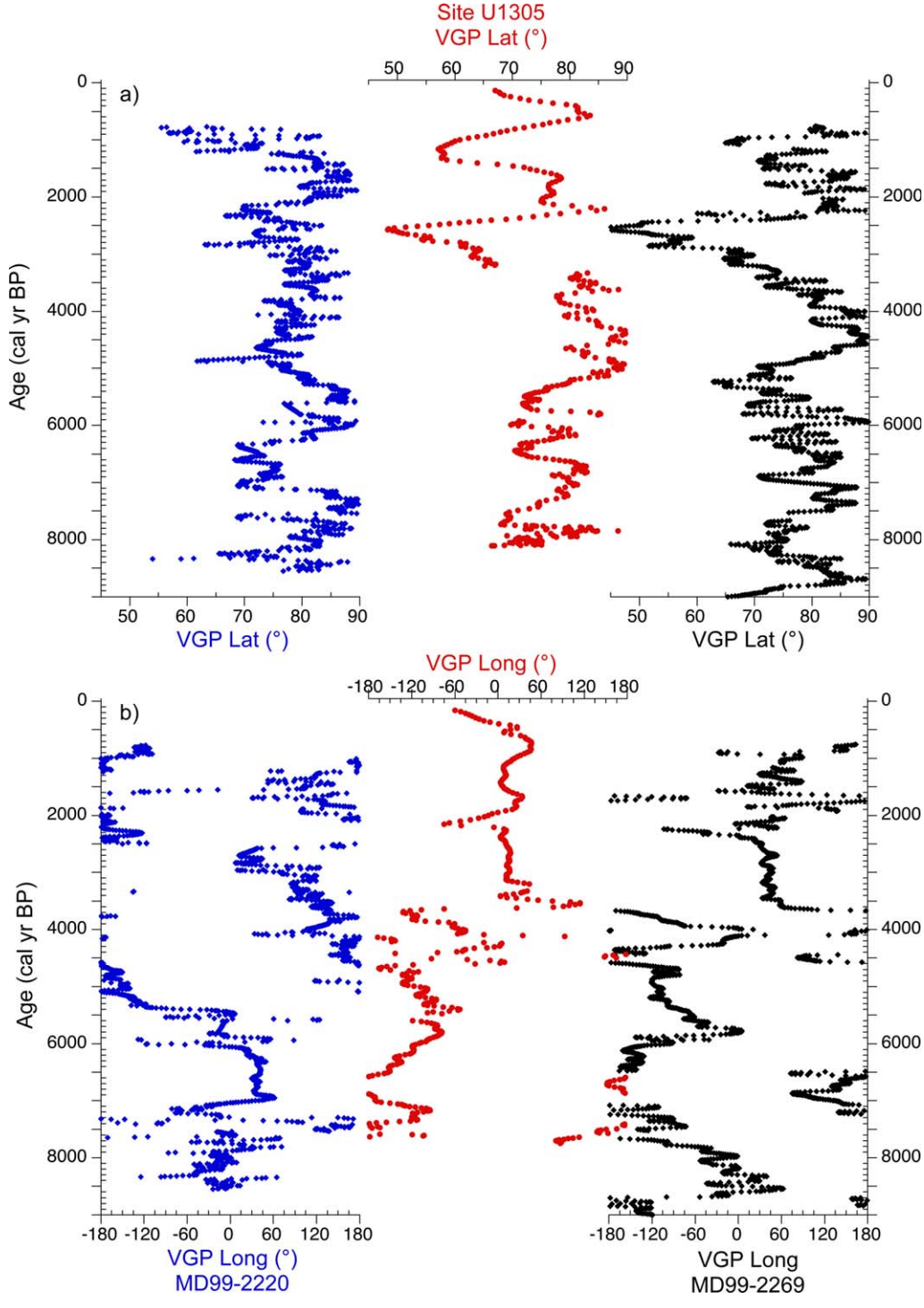

Figure 10. Comparison of PSV records expressed as virtual geomagnetic poles (VGP). (a) VGP latitude from left to right, core MD99-2220 (blue) [*St-Onge et al*., 2003], the upper 4.5 mcd of Site U1305 (red) on the tuned chronology as developed in Figure 8, and the Greenland/Iceland PSV composite (black). (b) VGP longitude from left to right, core MD99-2220 (blue) [*St-Onge et al*., 2003], the upper 4.5 mcd of Site U1305 (red) on the tuned chronology as developed in Figure 8, and the Greenland/Iceland PSV composite (black). For locations see Figure 1 and Table 1.

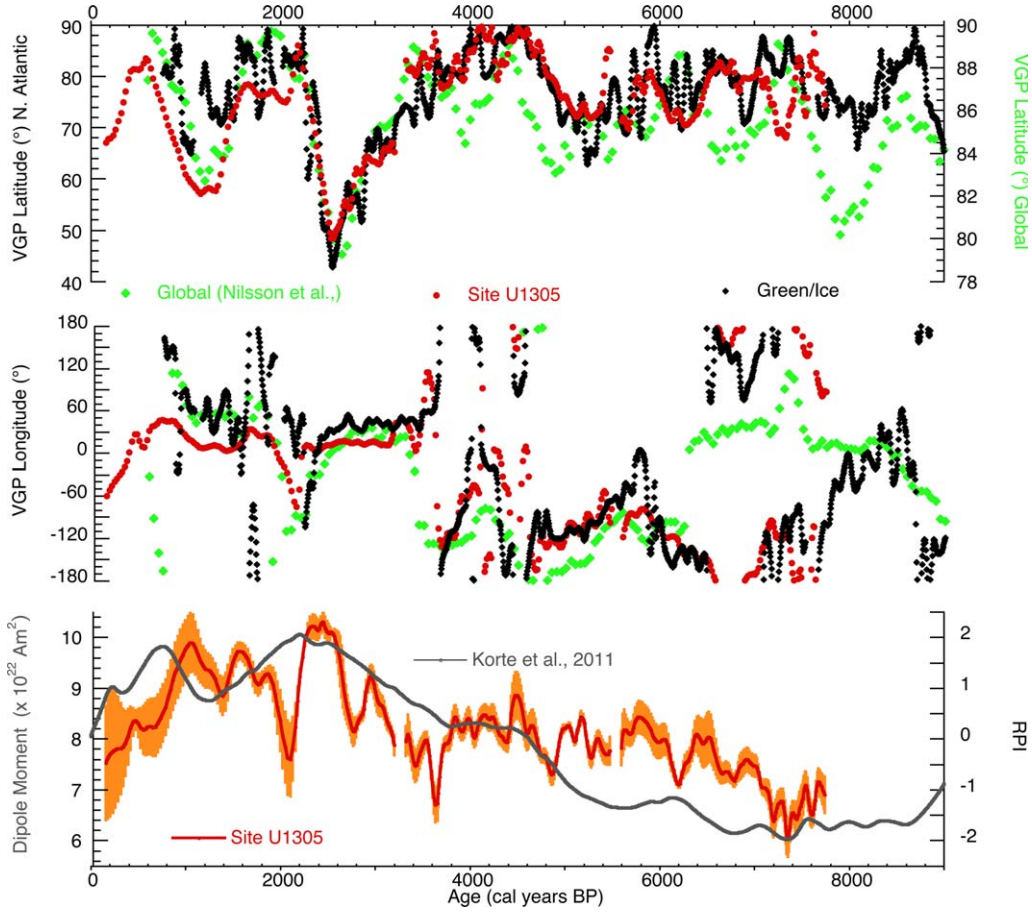

Figure 11. VGP comparison with global reconstructions and regional and global intensities. (a) VGP latitude from Site U1305 (red), Greenland/Iceland PSV composite (black), and *Nilsson et al*. [2011] global reconstruction FNBKE (green). (b) VGP longitude from Site U1305 (red), Greenland/Iceland PSV composite (black), and *Nilsson et al*. [2011] global reconstruction FNBKE (green). (c) Relative paleointensity from Site U1305 from Figure 9 (red) and the global dipole moment (dark green) [*Korte et al*., 2011].

lakes at around 2500 cal yrs BP [*Ólafsdóttir et al*., 2013] and exceptionally high VGP dispersion associated with Icelandic lavas [*Kristjansson and Jonsson*, 2007]. Archeomagnetic intensity compilations and CSHM [e.g., *Genevey et al*., 2008; *Knudsen et al*., 2008; *Donadini et al*., 2009; *Korte et al*., 2009, 2011] along with our results in Figures 11 and 12 show that North Atlantic, European, and apparently global intensities were high at this time, indicating that significant deviations from a GAD field are not limited to weak field conditions nor is a dominant GAD a prerequisite for high intensities [e.g., *Gallet et al*., 2009].

5.2. Influence of the High-Latitude Flux Lobes on the Northern North Atlantic PSV Record

[22] Historically persistent regions of concentrated geomagnetic flux at the core-mantle boundary (CMB), commonly known as flux lobes, are clearly observed at high-latitude locations in the northern hemisphere below Canada and Siberia [e.g., *Bloxham and Gubbins*, 1985; *Gubbins and Bloxham*, 1987; *Jackson et al*., 2000]. The persistence of these features is one of several lines of evidence suggesting that the geodynamo is influenced by the lower mantle [e.g., *Hide et al*., 1967; *Bloxham and Gubbins*, 1987; *Laj et al*., 1991; *Gubbins and Kelly*, 1993; *Johnson and Constable*, 1995; *Amit et al*., 2011]. The degree of this influence and how it manifests in PSV records on timescales slightly longer than historical is poorly understood and critically important to how we view the geodynamo [*Bloxham*, 2002; *Gubbins et al*., 2007; *Amit et al*., 2010]. By mapping the northern North Atlantic and global VGPs from Figure 11 on to the vertical component of magnetic field (Z) at the core-mantle boundary from 1590 to 1840 [*Gubbins et al*., 2006], we find that the VGPs are

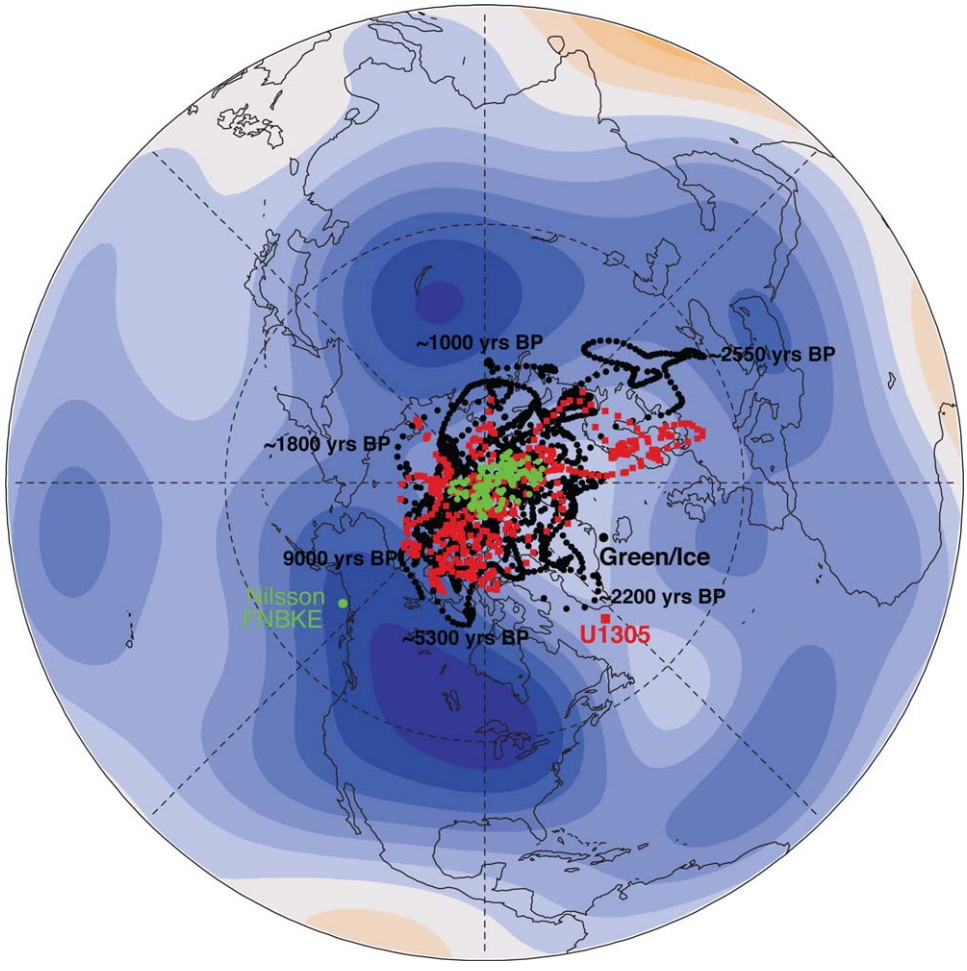

Figure 12. Virtual geomagnetic pole (VGP) positions from Site U1305 (red), Greenland/Iceland composite (black), and Global VGP reconstruction FNBKE (green) of *Nilsson et al*. [2011] as in Figure 11, overlain on vertical component of magnetic field (Z) on the core-mantle boundary in Lambert equal-area projection averaged over the interval 1590 to 1840 [after *Gubbins et al*., 2006]. Ages of a few selected Greenland/Iceland VGP features are shown.

bounded by both flux lobes and a third Euro/Mediterranean feature only hinted at from the historical record (Figure 12), but apparent in CSHMs over the last 3000 yrs [*Amit et al*., 2011]. The VGP time series in Figure 11 show how these patterns evolve with a shift from primarily North American to European longitudes at ~3500 cal yrs BP, and a shift back toward North American longitudes prior to the historical period. This shift toward European longitudes is accompanied by increased intensity, both in the North Atlantic and globally (Figure 11). Suggesting that the existence of an ephemeral Euro/Mediterranean VGP attractor (flux lobe?) could be important, not only to the PSV record in the North Atlantic (and elsewhere) but also to the high global field intensities that characterize the late Holocene [e.g., *McElhinny and Senake*, 1982; *Yang et al*., 2000; *Knudsen et al*., 2008; *Korte et al*., 2011].

[23] The exceptionally high amplitude of PSV in the northern North Atlantic, most clearly observed over the last 5 kyr at both Site U1305 and from the Greenland/Iceland composite, largely results from the high amplitude of declination (Figure 8). *Johnson and Constable* [1997] showed that declination at the Earth's surface reflects the radial magnetic field (B_r) at the CMB longitudinally peripheral to a site's location. In contrast, inclination and intensity at high northern latitudes reflect B_r at the CMB to the south of and centered around a site's location, respectively [e.g., *Johnson and Constable*, 1997; *Johnson and McFadden*, 2007]. Large shifts in northern North Atlantic declination would, therefore, result from B_r increases at the

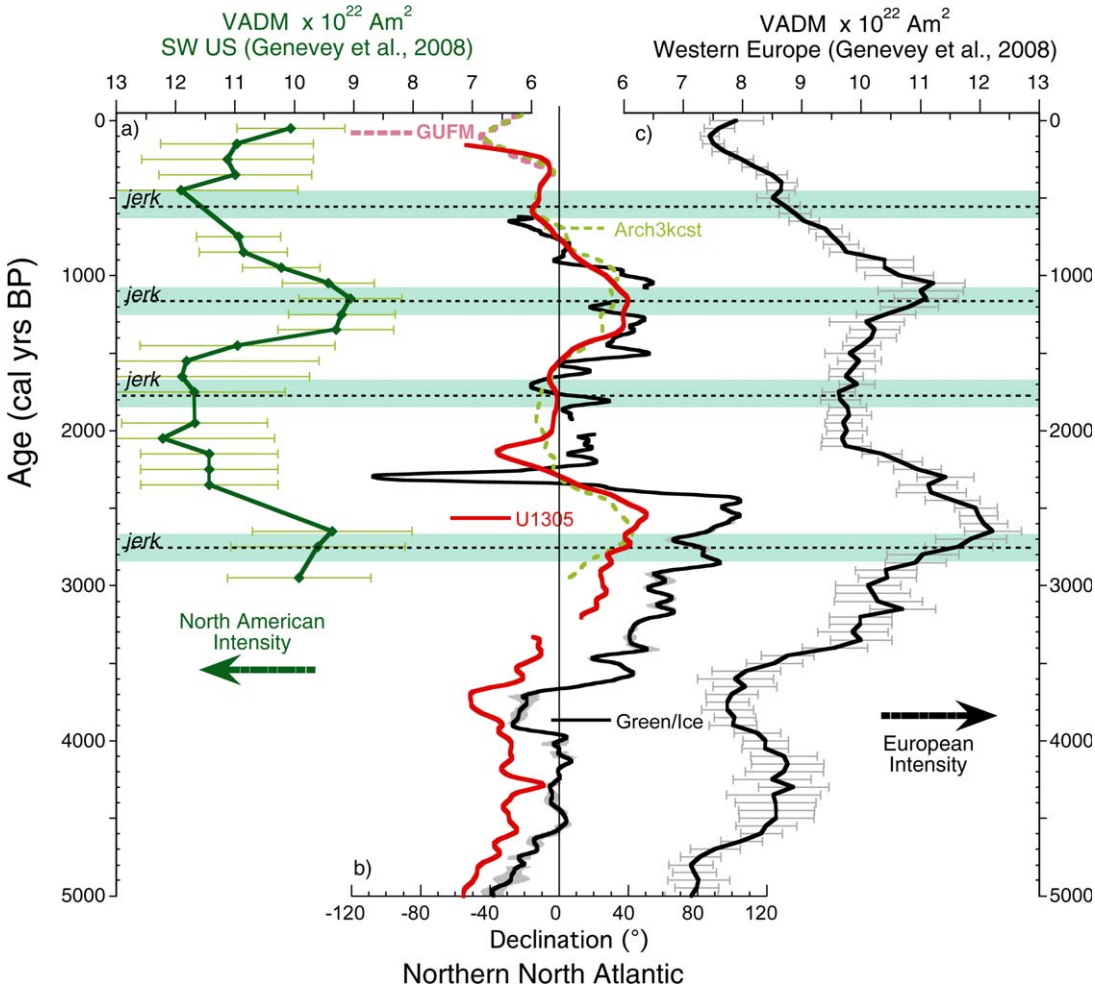

Figure 13. Intensity and PSV comparisons from North America to Europe: (a) Archeomagnetic intensity compilation (green, increasing to the left) from US Southwest [*Genevey et al*., 2008], (b) declination from Site U1305 (red) scaled to ARCH3k_cst.1 predictions [*Korte et al*., 2009] (stippled green), Greenland/Iceland PSV composite (black), and GUFM [*Jackson et al*., 2000] predictions (pink) overlain, and (c) European archeomagnetic intensity (black, increasing to right) [*Genevey et al*., 2008]. Horizontal lines indicate the timing of the archeomagnetic jerks of *Gallet et al*. [2003, 2009].

CMB to its east and west. As a stand in for such a direct comparison, in Figure 13, declination from the northern North Atlantic is compared with archeomagnetic intensities from North America and Europe. High intensities in North America are associated with westward declinations in the North Atlantic and low intensities in Europe, whereas this alternates with low intensities in North American, eastward declinations in the North Atlantic, and high intensities in Europe (Figure 13). Therefore, we argue that the high amplitude of PSV in the northern North Atlantic reflects its location relative to the generally out of phase centennial to millennial scale intensity oscillations in North America and Europe [e.g., *Lund and Schwartz*, 1999; *Gallet et al*., 2009].

[24] The past behavior of high-latitude flux lobes can in principle be at least partially observed through paleointensity reconstructions [*Gallet et al*., 2009]. Relative intensity highs, either in North America or Europe, and their associated northern North Atlantic declination anomalies, either eastward or westward, correspond to VGP latitude extrema and the timing of "archeomagnetic jerks" [*Gallet et al*., 2003] (Figures 11 and 13). Defined as sharp changes or cusps in directional drift and intensity maxima from European archeomagnetic data [*Gallet et al*., 2003], archeomagnetic jerks have been proposed as reflecting the development of a most eccentric (asymmetric) geomagnetic field resulting from the intensification of the high-latitude flux lobes [*Gallet et al*.,

2009]. Therefore, we hypothesize that Holocene PSV largely results from time varying flux concentrations oscillating between a few recurrent high-latitude locations. A "North American mode," characterized by high North American intensities, western North Atlantic declination, low European intensities, and GAD like VGPs (Figure 11) is more consistent with the time-averaged historical [e.g., *Jackson et al*., 2000], 10,000 year Holocene [e.g., *Korte et al*., 2011] and the 5 million year [*Gubbins and Kelly*, 1993] field models. Whereas a "European mode" characterized by relative lows in North American intensities, eastward North Atlantic declination, high European intensities, and lower latitude VGPs (Figures 11 and 13) are more consistent with time-averaged mid-to-late Holocene field [*Korte and Constable*, 2005] and much of the last 3000 yrs [*Amit et al*., 2011]. In this view, the present field appears to be in an interim state, heading from a North American and toward a European mode of variability.

6. Summary

[25] Site U1305 sediments preserve a high-quality paleomagnetic record of both directions and intensity that provide insights into the northern North Atlantic's paleogeomagnetic variability over the last 8000 yrs. Similarities with ultra-high resolution sediment records from very different environments, north Iceland and east Greenland continental margins [*Stoner et al*., 2007] and Icelandic lake [*Ólafsdóttir et al*., 2013], imply that the exceptionally high-amplitude PSV, as evidenced by apparently excursional VGP latitudes as recently as ~2500 yrs ago, are a robust determination of the region's paleogeomagnetic field, supporting the concept of persistent high amplitude PSV in the Atlantic region [e.g., *Gubbins and Gibbons* 2004].

[26] Detailed temporal comparisons show that the age of the magnetization in Site U1305 deep-sea sediments is younger than the age of the sediment, consistent with a pDRM process. This temporal offset and its depth equivalent can be estimated (-289 ± 77 yrs, 20 ± 5 cm) and corrected for under an assumption that ultra high-resolution sediments (e.g., Greenland/Iceland PSV composite) preserve a magnetization with negligible time-lag relative to its chronology. That these records accurately reflect the timing of the paleogeomagnetic field is at least partially tested through comparisons between Greenland/Iceland PSV composite and archeomagnetic predictions for the last 3000 yrs.

[27] Taken together, these high-resolution and well-dated paleomagnetic records allow us to place northern North Atlantic PSV and RPI into a regional context showing that the northern North Atlantic PSV and RPI are more consistent with European than North American records, and the evolution of VGPs are similar to global reconstructions, though with much larger latitudinal variations. The largest deviation from a geocentric axial dipole are observed during times of highest field intensities in the North Atlantic and globally. This suggests that directional PSV in the northern North Atlantic are a sensitive indicator of temporal oscillations of high-latitude flux concentrations (lobes) at a few recurrent locations as evidenced in global field models and regional paleointensity compilations. More work will be required to fully define these modes, their evolution, their geodynamo significance, and whether they reflect long-term persistence consistent with the idea that mantle heterogeneity has significant control on the geodynamo and the resulting behavior of the geomagnetic field.

Acknowledgments

[28] We would like to thank the Captain, crew of the RV JOIDES Resolution, the technical and support staff of the Integrated Ocean Drilling Program (IODP), the Expedition 303 Scientific Party, the staff of the Bremen Core Repository for allowing early sampling, W. M. Keck Carbon Cycle Accelerator Mass Spectrometry Laboratory at UC Irvine for AMS ^{14}C measurements, the Pacific NW Paleomagnetism Laboratory for hysteresis measurements, and Monika Korte for model predictions. We thank the United States Science Support Program and the US National Science Foundation grants OCE 0929066 (JSS) and OCE/EAR 088413/1014506 (JETC) for supporting this research. We acknowledge M. Davies and L. Ziegler for comments and careful reviews by four anonymous reviewers and T. Yamazaki. All data are available from the World Data Center for Paleoclimatology (http://www.ncdc.noaa.gov/paleo/paleo.html).

References

Alley, R. B., P. A. Mayewski, T. Sowers, M. Stuiver, K. C. Taylor, and P. U. Clark (1997), Holocene climatic instability: A prominent, widespread event 8200 yr ago, *Geology*, *25*, 483–486.

Amit, H., J. Aubert, and G. Hulot (2010), Stationary, oscillating or drifting mantle-driven geomagnetic flux patches?, *J. Geophys. Res.*, *115*, B07108, doi:10.1029/2009JB006542.

Amit, H., M. Korte, J. Aubert, C. Constable, and G. Hulot (2011), The time-dependence of intense archeomagnetic flux patches, *J. Geophys. Res.*, *116*, B12106, doi:10.1029/2011JB008538.

Banerjee, S. K., J. King, and J. Marvin (1981), A rapid method for magnetic granulometry with applications to environmental studies, *Geophys. Res. Lett.*, *8*(4), 333–336.

Barber, D. C., et al. (1999), Forcing of the cold event of 8,200 years ago by catastrophic drainage of Laurentide lakes, *Nature*, *400*, 344–348.

Barbetti, M., and M. McElhinny (1972), Evidence of a geomagnetic excursion 30,000 yr BP, *Nature*, *239*, 327–330.

Bard, E. (1988), Correction of accelerator mass spectrometry 14C ages measured in planktonic foraminifera: Paleoceanographic implications, *Paleoceanography*, *3*, 635–645.

Barletta, F., G. St-Onge, J. S. Stoner, P. Lajeunessse, and J. Locat (2010), A high-resolution Holocene paleomagnetic secular variation and relative paleointensity stack form eastern Canada, *Earth Planet. Sci. Lett.*, *298*, 162–174.

Bloxham, J. (2002), Time-independent and time-dependent behaviour of high-latitude flux bundles at the core-mantel boundary, *Geophys Res. Lett.*, *29*(18), 1854, doi:10.1029/2001GBLO14543.

Bloxham, J., and D. Gubbins (1985), The secular variation of Earth's magnetic field, *Nature*, *317*, 777–779.

Bloxham, J., and D. Gubbins (1987), Thermal core-mantle interactions, *Nature*, *325*, 511–513.

Brachfeld, S. A., and S. K. Banerjee (2000), A new high-resolution geomagnetic relative paleointensity record for the North American Holocene: A comparison of sedimentary and absolute intensity data, *J. Geophys. Res.*, *105*, 821–834.

Broecker, W. S., T. H. Peng, G. Ostlund, and M. Stuiver (1985), The DISTRIBUTION of bomb radiocarbon in the ocean, *J. Geophys. Res.*, *90*, 6953–6970.

Carlson, A., J. S. Stoner, J. Donnelly, and C. Hillaire-Marcel (2008), Response of the southern Greenland Ice Sheet during the last two deglaciations, *Geology*, *36*, 359–362.

Channell, J. E. T. (2006), Late Brunhes polarity excursions (Mono Lake, Laschamp, Iceland Basin and Pringle Falls) recorded at ODP Site 919 (Irminger Basin), *Earth Planet. Sci. Lett.*, *244*, 378–393.

Channell, J. E. T., and B. Lehman (1997), The last two geomagnetic polarity reversals recorded in high deposition-rate sediment drifts, *Nature*, *389*, 712–715.

Channell, J. E. T., and Y. Guyodo (2004), The Matuyama Chronozone at ODP Site 982 (Rockall Bank): Evidence for decimeter-scale magnetization lock-in depths, in *Timescales of the Paleomagnetic Field, Geophys. Monogr.*, vol. *145*, edited by J. E. T. Channell et al., AGU, Washington, D. C.

Channell, J. E. T, D. A. Hodell, and B. Lehman (1997), Relative geomagnetic paleointensity and $\delta^{18}O$ at ODP Site 983 (Gardar Drift, North Atlantic) since 350 ka, *Earth Planet. Sci. Lett.*, *153*, 103–118.

Channell, J. E. T, J. S. Stoner, D. A. Hodell, and C. D. Charles (2000), Geomagnetic paleointensity for the last 100 kyr from the sub-Antarctic South Atlantic: A tool for inter-hemispheric correlation, *Earth Planet. Sci. Lett.*, *175*, 145–160.

Channell, J. E. T., T. Kanamatsu, T. Sato, R. Stein, C. A. Alvarez Zarikian, M. J. Malone, and the Expedition 303/306 Scientists, North Atlantic Climate (2006), Proc. IODP, 303/306: College Station TX, Integrated Ocean Drilling Program Management International, Inc., doi:10.2204/iodp.proc.303306.2006.

Channell, J. E. T., C. Xuan, and D. A. Hodell (2009), Stacking paleointensity and oxygen isotope data for the last 1.5 Myr (PISO-1500), *Earth Planet. Sci. Lett.*, *283*, 14–23.

Colville, E. J., A. E. Carlson, B. L. Beard, R. G. Hatfield, J. S. Stoner, A. V. Reyes, and D. J. Ullman (2011), Extent of the southern Greenland Ice Sheet during the last interglacial, *Science*, *333*, 620–623.

Day, R., M. Fuller, and V. A. Schmidt (1977), Hysteresis properties of titanomagnetites: Grain-size compositional dependence, *Phys. Earth Planet. Inter.*, *13*, 260–267.

deMenocal, P. B., W. F. Ruddiman, and D. V. Kent (1990), Depth of post-depositional remanence acquisition in deep-sea sediments: A case study of the Brunhes Matuyama reversal and oxygen isotopic stage 19.1, *Earth Planet. Sci. Lett.*, *99*, 1–13.

Dergachev, V. A., O. M. Raspopov, B. van Geel, and G. I. Zaitseva (2004), The ''Sterno-Etrussa'' Excursion around 2700 BP and changes of the solar activity, cosmic ray intensity, and climate, *Radiocarbon*, *46*, 661–681.

de Vernal, A., and C. Hillaire-Marcel (2008), Natural variability of the Greenland climate, vegetation, and ice volume during the past million years, *Science*, *320*, 1622–1625.

Donadini, F., M. Korte, and C. G. Constable (2009), Geomagnetic field for 0–3 ka: 1. New data sets for global modeling, *Geochem. Geophys. Geosyst.*, *10*, Q06007, doi:10.1029/2008GC002295.

Dumberry, M., and C. C. Finley (2006), Eastward and westward drift of the Earth's magnetic field for the last three millennia, *Earth Planet. Sci. Lett.*, *254*, 146–157.

Dunlop, D. J., and B. Carter-Stiglitz (2006), Day plots of mixtures of superparamagnetic, single-domain, pseudo single-domain, and multidomain magnetites, *J. Geophys. Res.*, *111*, B12S09, doi:10.1029/2006JB004499.

Eirıksson, J., G. Larsen, K. L. Knudsen, J. Heinemeier, and L. A. Sımonarson (2004), Marine reservoir age variability and water mass distribution in the Iceland Sea, *Quat. Sci. Rev.*, *23*, 2247–2258.

Elsasser, W., E. P. Ney, and J. R. Winckler (1956), Cosmic-ray intensity and geomagnetism, *Nature*, *178*, 1225–1227.

Evans, H. F., J. E. T. Channell, J. S. Stoner, C. Hillaire-Marcel, J. D. Wright, L. C. Neitzke, and G. S. Mountain (2007), Paleointensity-assisted chronostratigraphy of detrital layers on the Eirik Drift (North Atlantic) since marine isotope stage 11, *Geochem. Geophys. Geosyst.*, *8*, Q11007, doi:10.1029/2007GC001720.

Expedition 303 Scientists (2005), *Site U1305, in Proc. IODP*, edited by J. E. T. Channell, et al., 303/305: College Station TX, Integrated Ocean Drilling Program Management International, Inc., doi:10.2204/iodp.proc.303305.105.2006.

Fagel, N., and C. Hillaire-Marcel (2006), Glacial/interglacial instabilities of the Western Boundary Under Current during the last 365 kyr from Sm/ND ratios of the sedimentary clay-size fractions at ODP site 646 (Labrador Sea), *Mar. Geol.*, *232*, 87–99.

Fagel, N., C. Hillaire-Marcel, and C. Robert (1997), Changes in the western boundary undercurrent outflow since the Last Glacial Maximum, from smectite/illite ratios in deep Labrador Sea sediments, *Paleoceanography*, *12*, 79–96.

Fagel, N., C. Innocent, C. Gariepy, and C. Hillaire-Marcel (2002), Sources of Labrador Sea sediments since the Last Glacial Maximum inferred from Nd-Pb isotopes, *Geochim. Cosmochim. Acta*, *66*, 2569–2581.

Fagel, N., C. Hillaire-Marcel, M. Humblet, R. Brasseur, D. Weis, and R. Stevenson (2004), Nd and Pb isotope signatures of the clay-size fraction of Labrador Sea sediments during the Holocene: Implications for the inception of the modern deep circulation pattern, *Paleoceanography*, *19*, PA3002, doi:10.1029/2003PA000993.

Gallet, Y., A. Genevey, and M. Le Goff (2002), Three millennia of directional variations of the Earth's magnetic field in western Europe as revealed by archeological artifacts, *Phys. Earth Planet. Inter.*, *131*, 81–89.

Gallet, Y., A. Genevey, and V. Courtillot (2003), On the possible occurrence of ''archaeomagnetic jerks'' in the geomagnetic field over the past three millennia, *Earth Planet. Sci. Lett.*, *214*, 237–242.

Gallet, Y., G. Hulot, A. Chulliat, and A. Genevy (2009), Geomagnetic field hemispheric asymmetry and archeomagnetic jerks, *Earth Planet. Sci. Lett.*, *284*, 179–186.

Genevey, A., Y. Gallet, C. G. Constable, M. Korte, and G. Hulot (2008) ArcheoInt: An upgraded compilation of geomagnetic field intensity data for the past ten millennia and its application to the recovery of the past dipole moment, *Geochem. Geophys. Geosyst.*, *9*, Q04038, doi:10.1029/2007GC001881.

Gubbins, D., and J. Bloxham (1987), Morphology of the geomagnetic field and implication for the geodynamo, *Nature*, *325*, 509–511.

Gubbins, D., and S. J. Gibbon (2004), Low Pacific secular variation, in *Timescales of the Paleomagnetic Field, Geophys. Monogr.*, vol. *145*, edited by J. E. T. Channell et al., pp. 279–286, AGU, Washington, D. C.

Gubbins, D., and P. Kelly (1993), Persistent patterns in the geomagnetic field during the last 2.5 Myr, *Nature*, *365*, 829–832.

Gubbins, D., A. L. Jones, and C. C. Finlay (2006), Fall in Earth's magnetic field is erratic, *Science*, *312*, 900–902.

Gubbins, D., A. P. Willis, and B. Sreenivasan (2007), Correlation of Earth's magnetic field with lower mantle thermal and seismic structure, *Phys. Earth Planet. Inter.*, *162*, 256–260.

Guyodo, Y., and J.-P. Valet (1996), Relative variations in geomagnetic intensity from sedimentary records: The past 200 thousand years, *Earth Planet. Sci. Lett.*, *143*, 23–26.

Guyodo, Y., and J.-P. Valet (1999), Global changes in intensity of the Earth's magnetic field during the past 800 kyr, *Nature*, *399*, 249–252.

Guyodo, Y., J. E. T. Channell, and R. Thomas (2002), Deconvolution of u-channel paleomagnetic data near geomagnetic reversals and short events, *Geophys. Res. Lett.*, *29*, 1845, doi:10.1029/2002GL014963.

Hagstrum, J. T., and D. E. Champion (2002), A Holocene paleosecular variation record from ^{14}C-dated volcanic rocks in western North America, *J. Geophys. Res.*, *107*(B1), doi:10.1029/2001JB000524.

Haltia-Hovi, E., N. Nowaczyk, and T. Saarinen (2010), Holocene palaeomagnetic secular variation recorded in multiple lake sediment cores from eastern Finland, *Geophys. J. Int.*, *180*, 609–622, doi:10.1111/j.1365-246X.2009.04456.x.

Herrero-Bervera, E., and J.-P. Valet (2007), Holocene paleosecular variation from dated lava flows on Maui (Hawaii), *Phys. Earth Planet. Inter.*, *161*, 267–280.

Hide, R. (1967), Motions of the Earth's core and mantle, and variations of the main geomagnetic field, *Science*, *157*, 55–56.

Hillaire-Marcel, C., and G. Bilodeau (2000), Instabilities in the Labrador Sea water mass structure during the last climatic cycle, *Can. J. Earth Sci.*, *37*, 795–809.

Hillaire-Marcel, C., A. de Vernal, S. Vallieres, and on board participants (1991), Cruise Report on On-Board Studies, CSS Hudson 91-045 GEOTOP-UQAM.

Hillaire-Marcel, C., A. De Vernal, G. Bilodeau, and G. Wu (1994a), Isotope stratigraphy, sedimentation rates, deep circulation, and carbonate events in the Labrador Sea during the last ~200 ka, *Can. J. Earth Sci.*, *31*, 63–89.

Hillaire-Marcel, C., A. De Vernal, M. Lucotte, A. Mucci, G. Bilodeau, A. Rochon, S. Vallieres, and G. Wu (1994b), Productivite et flux de carbone dans la mer du Labrador au cours des derniers 40 000 ans, *Can. J. Earth Sci.*, *31*, 139–158.

Hillaire-Marcel, C., A. De Vernal, G. Bilodeau, and A. J. Weaver (2001), Absence of deep-water formation in the Labrador Sea during the last interglacial period, *Nature*, *410*, 1073–1077.

Hillaire-Marcel, C., A. de Vernal, and D. J. W. Piper (2007), Lake Agassiz Final drainage event in the northwest North Atlantic, *Geophys. Res. Lett.*, *34*, L15601, doi:10.1029/2007GL030396.

Hillaire-Marcel, C., A. de Vernal, and J. McKay (2011), Foraminifer isotope study of the Pliestocene Labrador Sea, northwest North Atlantic (IODP Sites 1302/03 and 1305), with emphasis on paleoceanographical differences between its ''inner'' and ''outer'' basins, *Mar. Geol.*, *279*, 188–198.

Hunter, S., D. Wilkinson, E. Louarn, I. N. McCave, E. Rohling, D. A. V. Stow, and S. Bacon (2007), Deep western boundary current dynamics and associated sedimentation on the Eirik Drift, Southern Greenland Margin, *Deep Sea Res., Part I*, *54*, 2036–2066.

Irving, E., and A. Major (1964), Post-depositional detrital remanent magnetization in a synthetic sediment, *Sedimentology*, *3*, 135–143.

Jackson, A., A. R. T. Jonkers, and M. R. Walker (2000), Four centuries of geomagnetic secular variation from historical records, *Philos. Trans. R. Soc. London A*, *358*, 957–990.

Johnson, G. L., and E. D. Schneider (1969), Depositional ridges in the North Atlantic, *Earth Planet. Sci. Lett.*, *6*, 416–422.

Johnson, C. L., and C. G. Constable (1995), The time averaged geomagnetic field as recorded by lava flows over the past 5 Myr, *Geophys. J. Int.*, *122*, 489–519.

Johnson, C. L., and C. G. Constable (1997), The time-averaged geomagnetic field: Global and regional biases for 0–5 Ma, *Geophys. J. Int.*, *131*, 643–666.

Johnson, C. L., and P. McFadden (2007), Time-averaged field and paleosecular variation, in *Geomagnetism, Vol. 5 of Treatise on Geophysics*, edited by M. Kono and G. Schubert, pp. 417–453, Elsevier, Amsterdam.

Kawamura, N., N. Ishikawa, and M. Torii, (2012), Diagenetic alteration of magnetic minerals in Labrador Sea sediments (IODP Sites U1305, U1306, and U1307), *Geochem. Geophys. Geosyst.*, *13*, Q08013, doi:10.1029/2012GC004213.

King, J. W., S. K. Banerjee, J. A. Marvin, and Ö. Özdemir (1982), A comparison of different magnetic methods for determining the relative grain size of magnetite in natural materials: Some results from lake sediments, *Earth Planet. Sci. Lett.*, *59*, 404–419.

King, J. W., S. K. Banerjee, and J. Marvin (1983), A new rock-magnetic approach to selecting sediments for geomagnetic paleointensity studies: Application to paleointensity for the last 4000 years, *J. Geophys. Res.*, *88*, 5911–5921.

Kirschvink, J. L. (1980), The least squares lines and plane analysis of paleomagnetic data, *Geophys. J. R. Astron. Soc.*, *62*, 699–718.

Kleiven, H. F., C. Kissel, C. Laj, U. S. Ninnemann, T. O. Richter, and E. Cortijo (2008), Reduced North Atlantic deep water coeval with the Glacial Lake Agassiz freshwater outburst, *Science*, *319*, 60–64.

Knudsen, M. F., P. Rissager, F. Donadini, I. Snowball, R. Muscheler, K. Korhonen, and L. J. Pesonen (2008), Variations in the geomagnetic dipole moment during the Holocene and the past 50 kyr, *Earth Planet. Sci. Lett.*, *272*, 319–329.

Korte, M., and C. G. Constable (2003), Continuous global geomagnetic field models for the past 3000 years, *Phys. Earth Planet. Inter.*, *140*, 73–89.

Korte, M., and C. G. Constable (2005), Continuous geomagnetic field models for the past 7 millennia: 2. CALS7K, *Geochem. Geophys. Geosyst.*, *6*, Q02H16, doi:10.1029/2004GC000801.

Korte, M., and R. Holme (2010), On the persistence of geomagnetic flux lobes in global Holocene field models, *Phys. Earth Planet. Inter.*, *182*, 179–186.

Korte, M., and C. G. Constable (2011), Improving geomagnetic field reconstructions for 0–3 ka, *Phys. Earth Planet. Inter.*, *188*, 247–259.

Korte, M., A. Genevey, C. G. Constable, U. Frank, and E. Schnepp (2005), Continuous geomagnetic field models for the past 7 millennia: 1. A new global data compilation, *Geochem. Geophys. Geosyst.*, *6*, Q02H15, doi:10.1029/2004GC000800.

Korte, M., F. Donadini, and C. Constable (2009), Geomagnetic field for 0–3 ka: 2. Revised global time-varying models, *Geochem. Geophys. Geosyst.*, *10*, Q06008, doi:10.1029/2008GC002297.

Korte, M., C. G. Constable, F. Donadini, and R. Holme (2011), Reconstructing the Holocene geomagnetic field, *Earth Planet. Sci. Lett.*, *312*, 497–505.

Kristjansson, L., and G. Jonsson (2007), Paleomagnetism and magnetic surveys in Iceland, *J. Geodyn.*, *43*, 30–54, doi:10.1016/j.jog.2006.09.014.

Kristjansdottir, G. B., J. S. Stoner, A. Jennings, J. T. Andrews, and K. Grönvold (2007), Geochemistry of Holocene cryptotephras from the North Iceland Shelf (MD99-2269): Intercalibration with radiocarbon and paleomagnetic chronostratigraphies, *The Holocene*, *17*, 155–175.

Laj, C., and J. E. T. Channell (2007), Geomagnetic excursions, in *Treatise on Geophysics, vol. 5, Geomagnetism*, edited by M. Kono, pp. 373–416, Elsevier, Amsterdam.

Laj C., A. Mazaud, M. Fuller, and E. Herrero-Bervera (1991), Geomagnetic reversal paths, *Nature*, *351*, 11–26.

Laj, C., C. Kissel, A. Mazaud, J. E. T. Channell, and J. Beer (2000), North Atlantic paleointensity stack since 75 ka (NAPIS-75) and the duration of the Laschamp event, *Philos. Trans. R. Soc. London A*, *358*, 1009–1025.

Laj, C., C. Kissel, and J. Beer (2004), High resolution paleointensity stack since 75 kyr (GLOPIS-75) calibrated to absolute values, in *Timescales of the Paleomagnetic Field, Geophys. Monogr.*, vol. *145*, edited by J. E. T. Channell et al., pp. 255–265, AGU, Washington, D. C.

Laj, C., C. Kissel, and A. P. Roberts (2006), Geomagnetic field behavior during the Iceland Basin and Laschamp geomagnetic excursions: A simple transitional field geometry?, *Geochem. Geophys. Geosyst.*, *7*, Q03004, doi:10.1029/2005GC001122.

Lajeunesse, P., and G. St-Onge (2008), Subglacial origin of Lake Agassiz-Ojibway final outburst flood, *Nat. Geosci.*, *1*, 184–188.

Lucotte, M., and C. Hillaire-Marcel (1994), Inentification et distribution des grandes masses d'eau dans les mers du Labrador et d'Irminger, *Can. J. Earth Sci.*, *31*, 5–13.

Lund, S. P. (1996), A comparison of Holocene paleomagnetic secular variation records from North America, *J. Geophys. Res.*, *101*, 8007–8024.

Lund, S. P., and S. K. Banerjee (1985), Late Quaternary paleomagnetic field secular variation from two Minnesota Lakes, *J. Geophys. Res.*, *90*, 803–825.

Lund, S. P., and L. Keigwin (1994), Measurement of the degree of smoothing in sediment paleomagnetic secular variation records: An example from the late Quaternary deep-sea sediments of the Bermuda Rise, western North Atlantic Ocean, *Earth Planet. Sci. Lett.*, *122*, 317–330.

Lund, S. P., and M. Schwartz (1999), Environmental factors affecting geomagnetic field palaeointensity estimates from sediments, in *Quaternary Climates, Environments and Magnetism*, edited by B. A. Maher and R. Thompson, pp. 323–382, Cambridge, U. K.

Lund, S. P., M. Schwartz, L. Keigwin, and T. Johnson (2005), Deep-sea sediment records of the Laschamp geomagnetic field excursion (41,000 calendar years before present), *J. Geophys. Res.*, *110*, B04101, doi:10.1029/2003JB002943.

Lund, S., J. S. Stoner, G. Acton, and J. E. T. Channell (2006), Brunhes paleomagnetic field variability recorded in ocean drilling program cores, *Phys. Earth Planet. Inter.*, *156*, 194–204.

Mankinen, E. A., and D. E. Champion (1993), Latest Pleistocene and Holocene geomagnetic paleointensity on Hawaii, *Science*, *262*, 412–416.

Mazaud, A., and J. E. T. Channell (1999), The top Olduvai polarity transition at ODP Site 983 (Iceland Basin), *Earth Planet. Sci. Lett.*, *166*, 1–13.

Mazaud, A., C. Laj, and M. W. Bender (1994), A geomagnetic chronology for Antarctic ice accumulation, *Geophys. Res. Lett.*, *21*, 337–340.

Mazaud, A., J. E. T. Channell, C. Xuan, and J. S. Stoner (2009), Upper and lower Jaramillo polarity transitions recorded in IODP Expedition 303 North Atlantic sediments: Implications for transitional field geometry, *Phys. Earth Planet. Inter.*, *172*, 131–140.

Mazaud, A., M. A. Sicre, U. Ezat, J. J. Pichon, J. Duprat, C. Laj, C. Kissel, L. Beaufort, E. Michel, and J. L. Turon (2002), Geomagnetic-assisted stratigraphy and sea surface temperature changes in core MD94–103 (Southern Indian Ocean): Possible implications for North-South climatic relationships around H4, *Earth Planet. Sci. Lett.*, *201*, 159–170.

Mazaud, A., J. E. T. Channell, and J. S. Stoner (2012), Relative paleointensity and environmental magnetism since 1.2 Ma at IODP Site U1305 (Eirik Drift, NW Atlantic), *Earth Planet. Res. Lett.*, *357–358*, 137–144.

McElhinny, M. W., and W. E. Senanayake (1982), Variations in the geomagnetic dipole, 1. The past 50,000 years, *J. Geomagn. Geoelectr.*, *34*, 39–51.

Merrill, R. M., and P. McFadden (2003), The geomagnetic axial dipole field assumption, *Phys. Earth Planet. Inter.*, *139*, 171–185.

Merrill, R. M., M. W. McElhinny, and P. McFadden (1996), *The Magnetic Field of the Earth: Paleomagnetism, the Core and the Deep Mantle*, 531 pp., Academic, San Diego, Calif.

Nilsson, A., I. Snowball, R. Muscheler, and C. B. Uvo (2010), Holocene geocentric dipole tilt model constrained by sedimentary paleomagnetic data, *Geochem. Geophys. Geosyst.*, *11*, Q08018, doi:10.1029/2010GC003118.

Nilsson, A., I. Snowball, and R. Muscheler (2011), Millennial scale cyclicity in the geodynamo inferred from a dipole tilt reconstruction, *Earth Planet. Sci. Lett.*, *311*, 299–305.

Ólafsdóttir, S., Á. Geirsdóttir, G. H. Miller, J. S. Stoner, and J. E. T. Channell (2013), Synchronizing Holocene Lacustrine and marine sediment records in Iceland using paleomagnetic secular variation, *Geology*, *41*, 535–538, doi:10.1130/G33946.1.

Opdyke, N. D., and J. E. T. Channell (1996), *Magnetic Stratigraphy*, Academic, San Diego, Calif.

Paillard, D., L. Labeyrie, and P. Yiou (1996), Macintosh program performs time-series analysis, *Eos Trans. AGU*, *77*, 379.

Reimer, P. J., F. G. McCormac, J. Moore, F. McCormick, and E. V. Murray (2002), Marine radiocarbon reservoir

corrections for the mid- to late Holocene in the eastern subpolar North Atlantic, *The Holocene*, *12*, 129–135.

Reimer, P. J., et al. (2009), IntCal09 and Marine09 radiocarbon age calibration curves, 0–50,000 years cal BP, *Radiocarbon*, *51*, 1111–1150.

Rasmussen, S. O., et al. (2006), A new Greenland ice core chronology for the last glacial termination, *J. Geophys. Res.*, *111*, D06102, doi:10.1029/2005JD006079.

Raspopov, O. M., V. A. Dergachev, and E. G. Gooskova (2003), Ezekiel's vision: Visual evidence of Sterno-Etrussia geomagnetic excursion?, *Eos Trans. AGU*, *84*, 77, 83.

Ryan, W. B. F., et al. (2009), Global multi-resolution topography synthesis, *Geochem. Geophys. Geosyst.*, *10*, Q03014, doi:10.1029/2008GC002332.

Snowball, I., and P. Sandgren (2004), Geomagnetic field intensity changes in Sweden between 9000 and 450 cal BP: Extending the record of ''archaeomagnetic jerks'' by means of lake sediments and the pseudo-Thellier technique, *Earth Planet. Sci. Lett.*, *227*, 361–376.

Snowball, I., L. Zillen, A. Ojala, T. Saarinen, and P. Sandgren (2007), FENNOSTACK and FENNORPIS: Varve dated Holocene palaeomagnetic secular variation and relative paleointensity stacks for Fennoscandia, *Earth Planet. Sci. Lett.*, *255*, 106–116.

Srivastava, S. P., et al. (1987), *Proc. Init. Rep. (Pt. A)*, ODP, 105.

Stoner, J. S., J. E. T. Channell, C. Hillaire-Marcel, and J.-C. Mareschal (1994), High resolution rock magnetic study of a Late Pleistocene core from the Labrador Sea, *Can. J. Earth Sci.*, *31*, 104–114.

Stoner, J. S., J. E. T. Channell, and C. Hillaire-Marcel (1995a), Late Pleistocene relative geomagnetic paleointensity from the deep Labrador Sea: Regional and global correlations, *Earth Planet. Sci. Lett.*, *134*, 237–252.

Stoner, J. S., J. E. T. Channell, and C. Hillaire-Marcel (1995b), Magnetic properties of deep-sea sediments off southwest Greenland: Evidence for major differences between the last two deglaciations, *Geology*, *23*, 241–244.

Stoner, J. S., J. E. T. Channell, and C. Hillaire-Marcel (1996), The magnetic signature of rapidly deposited detrital layers from the deep Labrador Sea: Relationship to North Atlantic Heinrich layers, *Paleoceanography*, *11*, 309–325.

Stoner, J. S., J. E. T. Channell, and C. Hillaire-Marcel (1998), A 200 ka geomagnetic chronostratigraphy for the Labrador Sea: Indirect correlation of the sediment record to SPECMAP, *Earth Planet. Sci. Lett.*, *159*, 165–181.

Stoner, J. S., J. E. T. Channell, C. Hillaire-Marcel, and C. Kissel (2000), Geomagnetic paleointensity and environmental record from Labrador Sea Core MD95–2024: Global marine sediment and ice core chronostratigraphy for the last 110 kyr, *Earth Planet. Sci. Lett.*, *183*, 161–177.

Stoner, J. S., C. Laj, J. E. T. Channell, and C. Kissel (2002), South Atlantic (SAPIS) and North Atlantic (NAPIS) geomagnetic paleointensity stacks (0–80 ka): Implications for interhemispheric correlation, *Quat. Sci. Rev.*, *21*, 1142–1151.

Stoner, J. S., A. Jennings, G. B. Kristjansdottir, G. Dunhill, J. T. Andrews, and J. Hardardottir (2007) A paleomagnetic approach toward refining Holocene radiocarbon-based chronologies: Paleoceanographic records from the north Iceland (MD99-2269) and east Greenland (MD99-2322) margins, *Paleoceanography*, *22*, PA1209, doi:10.1029/2006PA001285.

St-Onge, G., J. S. Stoner, and C. Hillaire-Marcel (2003), Holocene paleomagnetic records from the St. Lawrence Estuary, Eastern Canada: Centennial to millennial-scale geomagnetic modulation of cosmogenic isotopes, *Earth Planet. Sci. Lett.*, *209*, 113–130.

Stuiver, M., P. J. Reimer, E. Bard, J. W. Beck, K. A. Hughen, B. Kromer, F. G. McCormack, J. van des Plicht, and M. Spurk (1998), INTCAL98 radiocarbon age calibration 24,000-0 cal. BP, *Radiocarbon*, *40*, 1041–1083.

Suganuma, Y., Y. Yokoyama, T. Yamazaki, K. Kawamura, C.-S. Horng, and H. Matsuzaki (2010), ^{10}Be evidence for delayed acquisition of remanent magnetization in marine sediments: Implication for a new age for the Matuyama–Brunhes boundary, *Earth Planet. Sci. Lett.*, *296*, 443–450.

Tauxe, L. (1993), Sedimentary records of relative paleointensity of the geomagnetic field: Theory and practice, *Rev. Geophys.*, *31*, 319–354.

Tauxe, L., and G. Wu (1990), Normalized remanence in sediments of the western Equatorial Pacific: Relative paleointensity of the geomagnetic field?, *J. Geophys. Res.*, *95*, 12,337–12,350.

Tauxe, L., and T. Yamazaki (2007), Paleointensities, in *Geomagnetism, vol. 5 of Treatise on Geophysics*, edited by M. Kono and G. Schubert, pp. 509–563, Elsevier, Amsterdam.

Tisnerat-Laborde, N., M. Paterne, B. Metivier, M. Arnold, P. Yiou, D. Blamart, S. Raynaud (2010), Variability of the northeast Atlantic sea surface Δ^{14}C and marine reservoir age and the North Atlantic Oscillation (NAO), *Quat. Sci. Rev.*, *29*, 2633–2646.

Thomas, R., Y. Guyodo, and J. E. T. Channell (2003), U-channel track for susceptibility measurements, *Geochem. Geophys. Geosyst.*, *4*, 1050, doi:10.1029/2002GC000454.

Thompson, R., and D. R. Baraclough (1982), Geomagnetic secular variation based on spherical harmonic and cross validation analyses of historical and archeomagnetic data, *J. Geomagn. Geoelectr.*, *34*, 245–263.

Thompson, R., and G. M. Turner (1979), British geomagnetic master curve 10,000-0 yr. B.P. for dating European sediments, *Geophys. Res. Lett.*, *6*, 249–252.

Torrence, C., and P. J. Webster (1999), Interdecadal changes in the ENSO-monsoon system, *J. Clim.*, *12*, 2679–2690.

Turon, J. L., C. Hillaire-Marcel, and Shipboard Participants (1999), Images V mission of the Marion Dufresne, 2nd leg, 30 June to 24 July 1999, Geol. Surv. Can., Open File 3782.

Valet, J. P. (2003), Time variations in geomagnetic intensity, *Rev. Geophys.*, *41*, 1004, doi:10.1029/2001RG000104.

Weeks, R. J., C. Laj, L. Endignoux, M. D. Fuller, A. P. Roberts, R. Manganne, E. Blanchard, and W. Goree (1993), Improvements in long core measurement techniques: Applications in palaeomagnetism and palaeoceanography, *Geophys. J. Int.*, *114*, 651–662.

Winsor, K., A. E. Carlson, G. P. Klinkhammer, J. S. Stoner, and R. G. Hatfield (2012), Evolution of the northeast Labrador Sea during the last interglaciation, *Geochem. Geophys. Geosyst.*, *13*, Q11006, doi:10.1029/2012GC004263.

Xuan, C., and J. E. T. Channell (2008), Origin of orbital periods in the sedimentary relative paleointensity records, *Phys. Earth Planet. Inter.*, *169*, 140–151.

Xuan, C., and J. E. T. Channell (2009), UPmag: MATLAB software for viewing and processing u channel or other pass through paleomagnetic data, *Geochem. Geophys. Geosyst.*, *10*, Q10Y07, doi:10.1029/2009 GC002584.

Yang, S., H. Odah, and J. Shaw (2000), Variations in the geomagnetic dipole moment over the last 12,000 years, *Geophys. J. Int.*, *140*, 158–162.

Ziegler, L. B., C. G. Constable, C. L. Johnson, and L. Tauxe (2011), PADM2M: A penalized maximum likelihood model of the 0–2 Ma paleomagnetic axial dipole moment, *Geophys. J. Int.*, *184*, 1069–1089.